Stimulation of voltage-dependent Ca^{2+} channels by NO at rat myenteric ganglia

MABRUKA S. H. SITMO
مبروكة صالح حمد سيتمو

INAUGURAL-DISSERTATION
zur Erlangung des Grades eines
Dr. med. vet.
beim Fachbereich Veterinärmedizin
der Justus-Liebig-Universität Gießen

édition scientifique
VVB LAUFERSWEILER VERLAG

1. Auflage 2009

1st Edition 2009

Printed in Germany

édition scientifique
VVB LAUFERSWEILER VERLAG

STAUFENBERGRING 15, D-35396 GIESSEN
Tel: 0641-5599888 Fax: 0641-5599890
email: redaktion@doktorverlag.de

www.doktorverlag.de

Aus dem Institut für Veterinär-Physiologie
der Justus-Liebig-Universität Gießen

Betreuer: Prof. Dr. Martin Diener

Stimulation of voltage-dependent Ca^{2+}channels by NO at rat myenteric ganglia

INAUGURAL-DISSERTATION
zur Erlangung des Grades eines
Dr. med. vet.
beim Fachbereich Veterinärmedizin
der Justus-Liebig-Universität Gießen

eingereicht von

Mabruka Sitmo

Tierärztin aus Elbaida-Libyen

Gießen 2009

Mit Genehmigung des Fachbereichs Veterinärmedizin
der Justus-Liebig-Universität Gießen

Dekan: Prof. Dr. Dr. habil. Georg Baljer

Gutachter: Prof. Dr. Martin Diener
Prof. Dr. Eberhard Burkhardt

Tag der Disputation: 06.02.2009

Table of Contents

Abbreviations

ACh	Acetylcholine
AP-1	Activating protein-1
AH	Afterhyperpolarization
BAPTA	1,2-bis(o-aminophenoxy)ethane-N,N,N',N'-tetraacetic acid
BSA	Bovine serum albumin
$[Ca^{2+}]_i$	Cytosolic free Ca^{2+} concentration
cAMP	Cyclic adenosine 3',5'-monophosphate
CCH	Carbachol
cDNA	Complementary deoxyribonucleic acid
cGMP	Cyclic guanosine 3',5'- monophosphate
CNS	Central nervous system
CPA	Cyclopiazonic acid
DAPI	4´,6-Diamidino-2-phenylindol dilactate
DEPC-water	Diethylpyrocarbonat-Aqua dest.
DHP	Dihydropyridine
DMEM	Dulbecco´s modified Eagle´s Medium
DMSO	Dimethylsulfoxide
dNTPs	Deoxynucleotide triphosphates
EGTA	Ethylene glycol-bis(β-aminoethyl ether)-N,N,N',N'-tetraacetic acid
eNOS	Endothelial nitric oxide synthase
ENS	Enteric nervous system
EPSPs	Excitatory postsynaptic potentials
ER	Endoplasmic reticulum
FCS	Fetal calf serum
Fura-2/AM	Fura-2-acetoxymethylester
GAPDH	Glycerinaldehyde-3-phosphate-dehydrogenase
GFAP	Glial fibrillary acidic protein
GI	Gastrointestinal tract
HEPES	N-(2-hydroxyethyl)-piperazine-N´-(2-ethanol sulfonic acid)
ICC	Interstitial cells of Cajal
IgG	Immunoglobuline
IGLE	Intraganglionic laminar endings
IL-1β	Interleukin-1β
IMAs	Intramuscular arrays
iNOS	Inducible nitric oxide synthase
IP_3	Inositol 1,4,5-trisphosphate
IPANs	Intrinsic primary afferent neurons
IPSPs	Inhibitory post-synaptic potentials
IP_3R	Inositol trisphosphate receptor
mRNA	Messenger ribonucleic acid
NADPH	Nicotinamide adenine dinucleotide phosphate
NANC	Non-adrenergic non-cholinergic

NF-κB	Nuclear factor κB
NO	Nitric oxide
NOS	Nitric oxide synthase
nNOS	Neuronal nitric oxide synthase
O_2^-	Superoxide anions
$ONOO^-$	Peroxynitrite anion
PAA	Phenylalkylamine
PB	Phosphate buffer
PBS	Phosphate-buffered saline
PBS-T	Triton-X-containing phoshate-buffered saline
PFA	Paraformaldehyde
PGP 9.5	Protein gene product 9.5
ROS	Reactive oxygene species
rpm	Rotations per minute
RT-PCR	Reverse transcriptase-Polymerase chain reaction
RYR	Ryanodine receptor
SEM	Standard error of the mean
SERCA	Sarcoplasmic-endoplasmic reticulum Ca^{2+}ATPase
SNP	Sodium nitroprusside
TAE	Tris-acetate/EDTA buffer
TNF-α	Tumor necrosis factor-α
TNFR	Tumor necrosis factor receptor
VDCCs	Voltage-dependent Ca^{2+} channels
VOCCs	Voltage-operated Ca^{2+} channels
V/V	Volume per Volume
W/V	Weight per Volume
λ	Wave length

1. Introduction

1.1. The myenteric plexus in the small intestine

The myenteric (Auerbach's) plexus is the outer of the two major plexuses of the enteric nervous system (ENS), which lies within the intestinal wall controlling several functions of the gastrointestinal tract (Costa et al. 2000, Figure 1).

The myenteric plexus is located between the longitudinal and the circular layers of the smooth muscle that form the gut's muscularis externa and regulates the motility (Gershon 1981). The plexus continues around and along the gut wall and has a connection with the other part of the enteric nervous system, i.e. the submucous plexus, which controls the transport of water and electrolytes across the intestinal epithelium (Furness and Costa 1987).

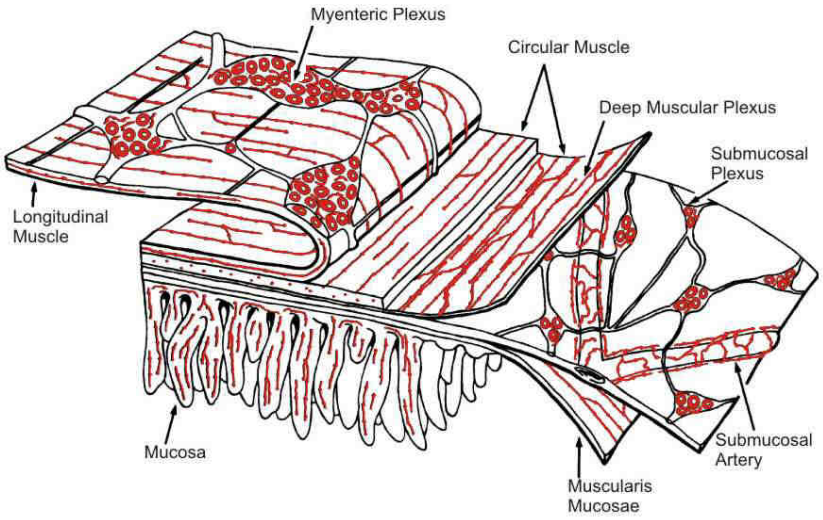

Figure 1.1: Schematic drawing of the enteric nervous system. Modified after Furness and Costa (1987).

Ultrastructure of enteric ganglia

The myenteric plexus consists of a network of nerve strands and small ganglia. The enteric ganglia, unlike other autonomic ganglia, do not contain blood vessels, connective tissue cells, or collagen fibers. The absence of connective tissue and the close packing of neurons and glia gives an appearance similar to the central nervous system. The ganglia are not encapsulated, but lie in the connective tissue between the muscle layers (Furness and Costa 1987).

The cells of the ganglia receive nutrients by diffusion from the blood vessels within the discontinuous basal lamina surrounding the ganglia. The neurons and their axons in the ganglion are partly surrounded by glial cells. The glial cells, which are histologically characterized by

gliofilaments, divide the neurites in the nerve strands to bundles (Gershon 1981).

1.2. Classification of myenteric neurons

Two types of myenteric neurons have been determined using the intracellular recording technique with microelectrodes. S/type1 cells have prominent fast excitatory postsynaptic potentials (fast EPSPs) and their action potentials are generated by the classic mechanism of activation and inactivation of time- and voltage-dependent Na^+ and K^+ channels (North 1982). The other type of myenteric neurons was termed AH/type2 cells, which do not show fast EPSPs. The action potential of these cells, at least at their soma, is carried by a Ca^{2+} current. This action potential is followed by a prolonged afterhyperpolarization (AH) generated by an outward Ca^{2+}-activated K^+ current, which lasts for up to 30 s (Nishi and North 1973, Hirst et al. 1974).

Morphologically, the ganglion cells in the myenteric plexus have been divided by the neuroanatomist Dogiel. Dogiel (1899) described type I cells as flattened cells with short dendrites and one axon. Type II cells possess an angular shape with many ramified dendrites. Type III cells are similar to the type II, but have more and shorter processes (Costa et al. 1986).

The electrophysiological identification of cells as the AH type was almost always corrrelated with a Dogiel type II morphology, whereas

cells electrophysiologically defined as S cells had in most cases a type I morphology (Bornstein et al. 1984). However, there are other neurons in the myenteric plexus, whose shape and electrophysiologic behavior do not fit to the previous classification (Wood 1994).

The functional classes of myenteric neurons are the intrinsic primary afferent neurons (IPANs), interneurons and motor neurons (Wood 1994). The IPANs respond to luminal chemical stimuli, to mechanical deformation of the mucosa and to stretch or tension of the muscle. This suggests the presence of processes of these cells into the mucosa (Hendriks et al. 1990, Costa et al. 2000). Intracellular microelectrode studies suggest that intrinsic primary afferent neurons are AH/Dogiel type II neurons (Kunze et al. 1998).

The interneurons represent the connection between the sensory and the motor neurons and form the information-processing circuitry of the myenteric plexus (Wood 1994). Interneurons have Dogiel type I (Kunze et al. 1998) and Dogiel type II morphology (Wood 1994). The motor neurons having Dogiel type I morphology represent the final motor output to the intestinal muscle. Both excitatory and inhibitory motor neurons are found in the myenteric plexus, which release neurotransmitters that cause contraction and inhibition of the contractile activity of the intestinal muscle, respectively (Wood 1994, Costa et al. 2000).

1.3. Synaptic events in myenteric neurons

The principal events found in the myenteric cells are fast excitatory postsynaptic potentials, slow excitatory postsynaptic potentials, slow inhibitory postsynaptic potentials and presynaptic inhibition of transmission from excitatory synapses (Furness and Costa 1987).

Fast excitatory postsynaptic potentials

Fast EPSPs are depolarizations of the membrane lasting less than 50 ms. They are found in S/type1 neurons and are rare in AH/type2 neurons (Wood 1984). Receptors directly coupled to nonspecific cation channels are involved in the mechanism of fast EPSPs (Derkach et al. 1989). The putative neurotransmitters involved in fast EPSPs are reported to be acetylcholine (ACh) and serotonin (5-HT) via 5-HT3 receptors.

Slow excitatory postsynaptic potentials

Prolonged depolarizations lasting for 5–20 s were shown in both S and AH neurons of the myenteric plexus (Katayama and North 1978). They are most pronounced in AH/type2 neurons, leading to a phase of hyperexcitability (Wood 1994). The slow EPSPs are associated with a reduction in membrane permeability to potassium ions (Wood and Mayer 1979), due to block of the Ca^{2+} channels by the neurotransmitter,

a reduction of the intraneural Ca^{2+} concentration and/or a closure of Ca^{2+}-activated K^{+} channels (Grafe et al. 1979). Experimental evidence suggested that cyclic AMP is involved in slow EPSPs of AH/type2 myenteric neurons (Nemeth et al. 1984). The putative neurotransmitters responsible for slow EPSPs are listed in Table 1.1.

Slow inhibitory postsynaptic potentials

Slow IPSPs are observed in a small proportion of myenteric neurons lasting for 2-40 s and are associated with an increase in potassium conductance (Johnson et al. 1980). Available evidence suggests that GTP-binding proteins are involved in direct coupling of the receptors to the potassium channels (Surprenant and North 1988). Norepinephrine is the putative neurotransmitter responsible for the slow IPSPs (Johnson et al. 1980). The functional significance of slow IPSPs is believed to be the termination of the excitatory state of slow synaptic excitation and reestablishment of the low excitability state in the ganglion cell soma (Wood 1994).

Presynaptic inhibition

The presynaptic inhibition is a mechanism that suppresses the release of neurotransmitters by an action of chemical messengers at receptors on the axons. It is found at both fast and slow excitatory and inhibitory synapses as well as at neuroeffector junctions (Schemann and Wood 1989). It functions to regulate the concentration of neurotransmitter within the synaptic or junctional space (Wood 1994).

Table 1.1. Some messenger substances found in myenteric neurons, enteroendocrine cells and immune cells of the gut.

Slow excitatory postsynaptic potentials	Slow inhibitory post-synaptic potentials	Presynaptic inhibition
Acetylcholine	Acetylcholine	Dopamine
Serotonin (5-HT)	Serotonin (5-HT)	Norepinephrine
Substance P	Enkephaline	Histamine
Histamin	Neurotensin	Serotonin (5-HT)
Vasoactive Intestinal Peptide(VIP)	Cholecystokinin	Opioid peptides
Cholecystokinin	Somatostatin	Acetylcholine
Gastrin-releasing peptide	Purines	Peptide YY
Bombesin	Galanine	Adenosine
Caerulein	Neuropeptide Y	Neuropeptide Y

1.4. The communication between the ENS and the central nervous system

The concept of autonomy of the ENS

The enteric nervous system of the gastrointestinal (GI) tract has traditionally been viewed as a system of ganglia that operates largely independently of the brain and the spinal cord. Because of this postulated autonomy, the ENS has even been characterised as the “little brain” in the gut. Recent neural tracing studies, however, challenge this canon of ENS autonomy (Powley 2000).

The prevailing view concerning vagal projections to the GI tract was established by Langley (Holst et al. 1997). Langley (1922) recognized the disparity between the few thousand preganglionic axons of the vagus and the millions of enteric neurons. Therefore, he hypothesized that vagal preganglionic neurons project to a few specialized postganglionic “vagal neurons” or “mother cells”, which, in turn, project divergently within the plexuses to coordinate autonomic control of the gut. This concept was reinforced by Bayliss and Starling's (1899) observation of organized propulsion of intraluminal boluses in intestinal segments removed from the body and studied in vitro (Langley and Magnus 1905). More recently, in a similar argument, Wood (1987) proposed that vagal parasympathetic preganglionic neurons project to selected “command neurons” located within the ENS (Holst et al. 1997).

Langley (1922) divided the autonomic nervous system into three divisions, an enteric, a sympathetic and a parasympathetic division.The enteric nervous system was classified as a separate autonomic entity because the bulk of enteric neurons were likely to receive no direct input from the central nervous system and could be accommodated in neither the sympathetic nor the parasympathetic definitions (Kirchgessner and Gershon 1989). Although the command neuron hypothesis has found wide acceptance, the supporting evidence for the concept is largely indirect and based primarily on the discrepancy between the number of preganglionic neurons or their axons and the number of enteric neurons to be innervated (Holst et al. 1997).

Recent neural tracing studies challenge this idea of complete ENS autonomy. Advances in neural tracing technologies have it made possible to collect structural observations that directly address the extent of the interconnections between the enteric and the central nervous system (Powley 2000). The observation of Kirchgessner and Gershon (1989) was consistent with the mother cell/command neuron concept, however, they stated: “despite the ability of the ENS to function independently of control by the CNS, it does not normally do so. The CNS affects the motility and secretory activity of the bowel” and refered to previous literature (Kerr and Preshaw 1969, Gonella et al. 1987, Roman and Gonella 1987). Other tracer and electrophysiological

experiments have revealed dense networks of preganglionic endings within ganglia with varicosities contacting large numbers of myenteric neurons (Berthoud et al. 1990, Schemann and Grundy 1992, Powley et al. 1994, Berthoud et al. 1995, Wang and Powley 2000).

1.5. Vagal input to the enteric nervous system of the small intestine

How do vagal fibers interact with intrinsic neurons to influence the output of effectors in the gut?

The vagus nerve supplies the majority of the visceral afferents that allow the central nervous system to coordinate the functions of the gut (Fox et al. 2000). Prechtl and Powley (1990) have demonstrated that 70 – 80 % of the fibers in the abdominal vagus are sensory. The vagus nerve contains both sensory and motor axons that have been implicated in the control of gastrointestinal physiology and ingestive behavior (Phillips et al. 1997). The vagal afferents are classified as mechanoreceptors and chemoreceptors (Grundy and Scratcherd 1989). Three types of vagal mechanoreceptors have been identified on the basis of their location, morphology and electrophysiologic properties (Powley and Phillips 2002). One of them are the intraganglionic laminar endings (IGLE), which lie parallel to the muscle layers and interact with both neural and connective tissue elements around myenteric ganglia (Nonidez 1946, Rodrigo et al. 1975). IGLEs are well organized to detect contraction-

related tension and other distortion for purpose of coordinating the rhythmic motor patterns of the gut such as peristalsis (Fox et al. 2000). The second type of vagal afferents found in the smooth muscle of the intestine are the intramuscular arrays (IMAs) located within the circular and longitudinal muscle sheets. They run parallel to the smooth muscle fibers of the muscular sheet and form appositions with interstitial cells of Cajal (Berthoud and Powley 1992, Wang and Powley 1994). On the basis of their morphology and distribution within the muscle wall, IMAs appear to be specialized to operate as stretch receptors that are capable of transducing changes in the length of their respective muscle sheets (Wang and Powley 2000). IGLEs are widley distributed in the initial segment of the duodenum. Their density is reduced in the distal small intestine. The third type of vagal mechanoreceptors has been identified electrophysiologically and is postulated to act as mucosal mechanoreceptors (Powley and Phillips 2002).

Vagal chemoreceptors are distributed in the lamina propria. They are situated among the intestinal crypts, they enter and ramify in individual villi of the mucosa and end near the basal side of the epithelial cells (Berthoud et al. 1995). The chemoreceptors are sensitive to all three macronutrients and to changes in pH and osmolarity within the intestinal lumen (Mei 1985, Ritter et al. 1992). Mucosal terminals are abundant in the proximal duodenum, becoming relatively sparse in the distal small

intestine (Williams et al. 1997). The extensive distribution of vagal afferents in this region points to the importance of the proximal duodenum in the detection of nutrients, distension and hormones and thus the important role in the feedback control of gastric activity as well as feeding behavior (Hölzer and Raybould 1992, Smith et al. 1994, Walls et al. 1995).

1.6. Modulation of the enteric nervous system by the central nervous system

The digestive tract is endowed with an enteric nervous system capable of integrating a substantial volume of local neural, hormonal and immune afferent signal data (Wood 1984). Nevertheless, this enteric neural network acts principally as a local controller of digestive organ functions subject to descending neural control from the CNS (Wood 1987). Vago-vagal reflexes, and the factors that modulate their functions, represent the next hierarchy in the coordinated neural control of the entire digestive tract (Powley et al. 1994).

The exact role of both CNS and ENS in the control of GI tract motility used to be a matter of controversy. Some investigators have defined the peristalsis reflex as a local reflex with intrinsic afferent neurons in the myenteric plexus independent of the extrinsic nerve supply to the GI tract (Wood 1984). Others have implied a role of the vagal afferents in the reflex (Powley 2000). However, Grider and Jin (1994) indicated that

sensory neurons activated by mucosal stimulation are wholly intrinsic, whereas sensory neurons activated by muscle stretch are extrinsic with cell bodies in the CNS.

How the vagal fibers interact with intrinsic neurons to influence the output of effectors in the gut has not yet been demonstrated (Kirchgessner and Gershon 1989), however, some investigators have reported the presence of CGRP (calcitonin-gene related peptide) and substance P in the axons of the vagal afferents which synapse with the myenteric neurons (Berthoud and Neuhuber 2000, Powley 2000). At the level of the efferent fibers, subsets of myenteric neurons containing 5-HT and VIP have been described (Kirchgessner and Gershon 1989).

1.7. Sympathetic influence on gastrointestinal function

The primary adrenergic innervation of the small intestine is located at the myenteric plexus. The sympathetic innervation of the smooth musculature is relatively sparse suggesting that the adrenergic inhibiting mechanism takes place primarily at the myenteric ganglia (Jacobowitz 1965).

The adrenergic inhibition of the intestinal motility is by acting on the excitatory pathway through the enteric cholinergic neurons (Jansson and Martinson 1966) and/or on the extrinsic excitatory parasympathetic nervous activity (Lundgren 2000). Pharmacological studies have shown that noradrenergic nerve fibers cause a presynaptic inhibition of

acetylcholine release from enteric excitatory motor cholinergic neurons mediated through α-receptors (Drew 1978).

The noradrenergic nerves innervating the intestine usually are inactive in the resting individual. Their discharge is evoked through reflex pathways originating both out- or inside the gastrointestinal tract (Furness and Costa 1987). The intestino-intestinal reflexes which are evoked by distension or mucosal irritation of one part of the intestine can inhibit the movement of other areas involving spinal and prevertebral pathways (Kuntz and Saccomanno 1944). Pilipenko (1956) found that the intestinofugal fibers that arise from the myenteric nerve cells are involved in the peripheral intestino-intestinal inhibitory reflex evoked by noxious stimuli. For example rough handling of the viscera inhibits the motor activity of the intestine through the action of noradrenergic nerves to inhibit the activity of the enteric neurons (Furness and Costa 1987). The sympathetic pathway to the intestine encodes information above supraphysiological levels of intestinal pressure and forms the main pathway for mediating pain perception (Grundy 2002).

Overall, the intestinal motor activity is controlled by the enteric nervous system, which itself is influenced by extrinsic nerves. The importance of the ENS in motor functions is illustrated by the obstruction when a segment of bowel is congenitally deprived of ganglion cells, as occurs in Hirschsprung´s disease (Bodian et al. 1949) and the motor dysfunction

after small bowel transplantation reflects the importance of the extrinsic innervation to the gut (Nakao et al. 1998).

1.8. Nitric oxide

Nitric oxide (NO) is an inorganic gaseous molecule that acts as an inhibitory neurotransmitter in the enteric nervous system. NO has been identified to be identical to the endothelium-derived relaxing factor discovered by Furchgott and Zawadzki (Palmer et al. 1987). This gas plays an important role in the non-adrenergic and non-cholinergic (NANC) neurotransmission in the intestine (Calignano et al. 1992) and it has been shown to act as an inhibitory neurotransmitter of interneurons (Wiklund et al. 1993) as well as of motor neurons innervating the intestinal muscle (Sanders and Ward 1992). NO has been determined to be involved in the descending inhibitory component of the peristaltic reflex in the GI tract (Costa et al. 1991). Nitric oxide is produced by the enzyme nitric oxide synthase (NOS), which catalyzes the conversion of L-arginine to L-citrulline and NO (Moncada et al. 1991). The mechanism by which NO is synthesized is NADPH- and Ca^{2+}/calmodulin-dependent (Palmer and Moncada 1989, Busse and Mulsch 1990).

Three isoforms of NOS have been detected (Dawson et al. 1991), the neuronal (n)NOS (NOS-1) and the endothelial (e)NOS (NOS-3) are constitutively expressed and are Ca^{2+}-dependent, while the inducible (i)NOS (NOS-2) is Ca^{2+}-independent. The neuronal and endothelial

isoforms occur under physiological conditions, whereas the inducible isoform is expressed e.g. in macrophages after activation by endotoxins and cytokines (Cattel and Janson 1995). However, iNOS activity has been reported in the gastrointestinal tract both under physiological as well under pathological conditions (Mancinelli et al. 2001). Besides enteric neurons, the interstitial cells of Cajal (ICC) and the smooth muscle cells seem to be able to express nNOS (Daniel et al. 2000, Wang et al. 2000).

Due to its gaseous nature, NO does not need a classical release machinery, but is synthesized on demand and can easily diffuse from the producing cells into the target effector cells (Garthwaite et al. 1988). However, some evidences suggest that NO can be stored in form of nitrosothiols after binding at thiol containing amino acids (Thornbury et al. 1991).

Nitric oxide exerts its action via activation of soluble guanylate cyclase and subsequent elevation of the second messenger guanosine 3',5'-cyclic monophosphate (cGMP; Arnold et al. 1977), however, there have been reports of NO actions that are non-cGMP dependent (Garg and Hassid 1991).

NO binds to iron in a heme moiety that is attached to guanylate cyclase and activates the enzyme. The consequence is a production of cGMP and the activation of a cGMP-dependent protein kinase, which may e.g. activate Ca^{2+}-activated K^{+} channels responsible for the inhibitory

junction potential and relaxation of the intestinal muscle (Lang et al. 2000), or may decrease the Ca^{2+} sensitivity of the contractile apparatus (Thornbury et al. 1991).

Furthermore, NO has been identified to modify cellular proteins by S-nitrosylation. The coupling of NO to the thiol side chain of cysteins to form an S-nitrosothiol seems to be an important mechanism for post-translational regulation of most or all main classes of proteins (Hess et al. 2005). In addition, formation of peroxynitrite anion ($ONOO^-$) through reaction of NO with superoxide (O_2^-) is implicated in NO-mediated cytotoxicity and may be involved in NO mediated immune responses by macrophages under pathological conditions (Beckman and Koppenol 1996).

NO has been found to have a role as presynaptic inhibitory modulator on acetylcholine and on substance P release from myenteric neurons of the guinea-pig small intestine (Wiklund et al. 1993, Kilbinger and Wolf 1994).

1.9. Interstitial cells of Cajal and NO

Intestinal muscle possesses a mechanism for the self-generation of rhythmic changes in excitability (periodic depolarizations). The movement of the intestine depends on the superimposition of the action of nerves and hormones on this underlying rhythm, which are referred to as slow waves. They last from 2 to 5 s, have a variable amplitude (up to

20 mV), and occur at frequencies from 3 to 30 per min depending on the species and the region of gastrointestinal tract (Furness and Costa 1987).

The interstitial cells of Cajal (ICs) are the initiators of slow waves in the gastrointestinal tract (Thuneberg 1982). In addition to the role of ICs in generation of pacemaking, they serve as the mediator of certain forms of enteric motor neurotransmission (Sanders 1996).

Interstitial cells have been found at the level of myenteric plexus (IC-MP), in the muscle layers (IC-CM; IC-LM) and in the deep muscular plexus (IC-DMP) (Jiménez et al. 1999) forming synapse-like contacts with myenteric neurons (Ward 2000). IC-MP are thought to be involved in the generation of slow waves. IC-IMs and IC-DMP probably serve as mediators of neurotransmission (Horiguchi et al. 2003). Smith et al. (1989) reported that the inhibitory innervation of the gastrointestinal muscle is concentrated in regions, where ICs are located, and isolated ICs have been shown to be responsive to NO by changes in cellular levels of cGMP (Young et al. 1993). Furthermore, fibers of enteric neurons with NOS immunoreactivity that are closely associated with the cell bodies of ICs have been determined (Ward 2000).

Impairment of ICs-mediated control of electrical events and neuromodulation has been implicated in several motility disorders such as grass sickness in horses and Crohn's disease in human (Ward et al. 1994, Altdorfer et al. 2002). Increased NOS immunoreactivity in ICs

during inflammation may contribute to the motility disorders (Altdorfer et al. 2002).

1.10. Calcium signaling in myenteric neurons

Calcium plays an important role in the regulation of a great variety of neuronal processes including neurotransmission, excitability, regulation of enzymatic activities or gene expression (Berridge 1998). Like other cells, the free cytosolic Ca^{2+} concentration of neuronal cells is kept low by a series of plasma membrane pumps or exchangers and several intracellular Ca^{2+} sequestering units such as endoplasmic reticulum (ER) and mitochondria (Kennedy 1989, Figure 1.2).

The neuronal endoplasmic reticulum contributes to the Ca^{2+} signaling by acting either as a source or as a sink of Ca^{2+} (Miller 1991, Berghe et al. 2002). The ER is a continuous membrane network that extends throughout the neuron and interacts with the plasma membrane to control a wide range of neuronal processes (Berridge 1998).

Ca^{2+} is released from the ER upon activation of either the inositol 1,4,5-trisphosphate (IP_3) receptors (IP_3Rs) or the ryanodine receptors (RYRs; Simpson et al. 1995). These receptors are sensitive to Ca^{2+} and display the phenomenon of Ca^{2+}-induced Ca^{2+} release, which is responsible for amplifying Ca^{2+} signals from the outside. The entry of Ca^{2+} from the outside is regulated by voltage-operated channels (VOCCs) or by receptor-operated channels. Metabotropic neurotransmitters stimulate

the formation of IP_3, which acts on IP_3Rs to release Ca^{2+} from the ER (Berridge 1998). The ryanodine receptors are sensitive to the second messenger cyclic ADP ribose, which enhances Ca^{2+} release (Galione 1994).

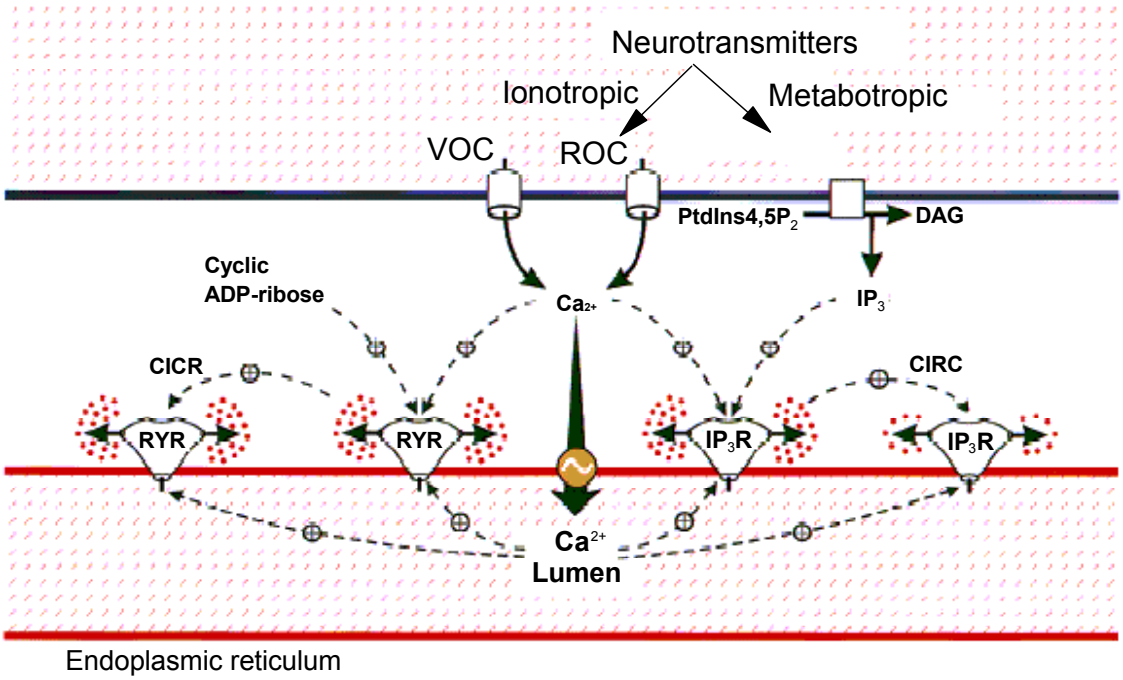

Figure 1.2: Neuronal calcium signaling (from Berridge 1998). VOC = voltage operated channel; ROC = Receptor operated channel; PtdIns4,5P_2 = Phosphatidylinositol 4,5-biphosphate; DAG = Diacylglycerol; IP_3 = inositol 1,4,5-trisphosphate; IP_3R = inositol trisphosphate receptor; RYR = Ryanodine receptor; CICR = Calcium-induced calcium release; Ca^{2+} = Calcium ions.

The role of Ca^{2+} in modulation of neuronal excitability is mediated by changes in the membrane potential. The afterhyperpolarization (AH), which has been identified in myenteric neurons to regulate the rate of firing by interrupting high frequency discharges, arises from the opening

of Ca^{2+}-activated K^+ channels; the underlying rise of the cytosolic Ca^{2+} concentration is mediated by an influx into the cell via VOCCs and/or a release of stored Ca^{2+} from the ER (Berridge 1998). However, Ca^{2+} has also been implicated in depressing neuronal activity. Modification in the amplitude, or spatial and temporal presentation of Ca^{2+} signals may account for this.

A localized rise in the Ca^{2+} concentration can originate from channels in the plasma membrane or on the internal stores. These signals can either activate highly localized cellular processes in the immediate vicinity of the channels or produce a Ca^{2+} wave that spreads throughout the cell to activate processes at a global level. This phenomenon may explain how Ca^{2+} signals arising locally near the plasma membrane activate potassium channels and cause the muscle to relax, whereas elementary release events deeper in the cell create global Ca^{2+} signals and then the muscle contracts (Berridge et al. 1998).

Since my work deals with the effect of NO on myenteric neurons with regard to voltage-operated calcium channels, these channels are described in more detail below.

Voltage operated calcium channels

Voltage-operated calcium channels mediate Ca^{2+} entry into cells in response to membrane depolarization and they are the signal transducers that convert electrical signals in the cell membrane into an

increase in the concentration of the intracellular second messenger Ca^{2+} (Catterall 2000). Multiple types of Ca^{2+} currents have been identified by their physiological and pharmacological properties and have been correlated with cloned Ca^{2+} channel subunits characterized by expression in vitro (Catterall 2000). The Ca^{2+} channels that have been characterized biochemically are complex proteins composed of four or five distinct subunits. The amino acid sequence of the $\alpha 1$ subunit is organized in four repeated domains (I-IV), each of which contains six transmembrane segments (S1-S6), and a membrane associated loop between the transmembrane segments S5 and S6. The S4 segments of each homologous domain serve as voltage sensors for activation, moving outward and rotating under the influence of the electric field and initiating a conformational change that opens the pore. The S5 and S6 segments and the membrane-associated pore loop between them forms the pore lining of the voltage-gated ion channels. The narrow external pore is lined by the pore loop and is responsible for Ca^{2+} selectivity. The inner pore is lined by the S6 segments, which form the binding sites for the pore-blocking Ca^{2+} antagonists. An intracellular β-subunit and a transmembrane, disulfide-linked $\alpha 2\delta$-subunit complex are component of most types of Ca^{2+} channels. A γ-subunit has also been found in skeletal muscle Ca^{2+} channels and related subunits are expressed in heart and brain (Catterall 2000).

Although these auxillary subunits modulate the properties of the channel complex, the pharmacological and electrophysiological diversity of Ca^{2+} channels arises primarily from the existence of multiple α1-subunits (Hofmann et al. 1994). Mammalian α1 subunits are encoded by at least ten distinct genes and are grouped into three subfamilies. The Ca_v1 subfamily ($Ca_v1.1$ to $Ca_v1.4$) includes channels containing α1C, α1D, α1F, α1S, which mediate L-type Ca^{2+} currents in different tissues. The Ca_v2 subfamily ($Ca_v2.1$ to $Ca_v2.3$) includes channels containing α1A, α1B, α1E, which mediate P/Q-,N-, and R-type Ca^{2+} currents, respectively. The Ca_v3 subfamily ($Ca_v3.1$ to $Ca_v3.3$) includes channels containing α1G, α1H, α1I, which mediate T-type Ca^{2+} currents (Catterall et al. 2003).

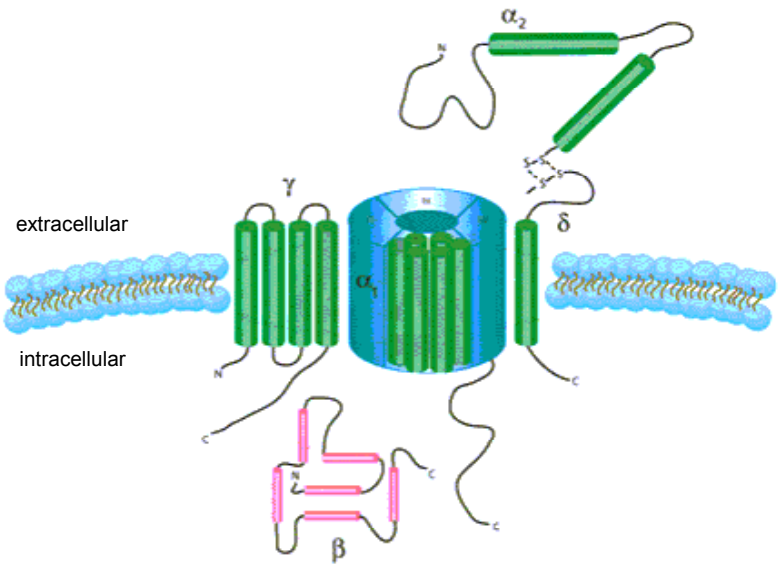

Figure 1.3: Transmembrane organization of the calcium channel subunits (from: www.sigmaaldrich.com).

Calcium currents have diverse physiological and pharmacological properties. L-type Ca^{2+} currents require a strong depolarization for activation, are long lasting and are blocked by the organic antagonists dihydropyridines and phenylalkylamines (Sher et al. 1991). L-type Ca^{2+} currents in neurons are important in regulation of gene expression and in integration of synaptic inputs (Bean 1989). N-type, P/Q-type, and R-type Ca^{2+} currents also require strong depolarization for activation. They are insensitive to L-type Ca^{2+} channel blockers, but are blocked by specific polypeptide toxins from snail and spider venoms. They initiate neurotransmission at synapses and mediate calcium entry into cell bodies and dendrites (Catterall et al. 2003). The low voltage-activated T-type Ca^{2+} currents develop only transiently and are resistant to both organic antagonists and to the snake and spider toxins. They are involved in shaping the action potential and controlling patterns of repetitive firing (Catterall et al. 2003).

The presence of these types of VOCCs was shown in myenteric neurons immunohistochemically (Kirchgessner and Liu 1999) and pharmacologically in rat and guinea pig small intestine (Schäufele and Diener 2005, Bian et al. 2004).

Nitric oxide has been identified to be one of the key messengers govering the overall control of Ca^{2+} homeostasis in a number of cell systems (Clementi 1998). Several evidences have indicated that NO

affects Ca^{2+} signalling via different pathways. Release of Ca^{2+} from intracellular stores by action of NO has been defined. For example, in hepatocytes NO activates IP_3 receptors via G-kinase phosphorylation of these receptors leading to release Ca^{2+} from the endoplasmic reticulum (Rooney et al. 1996). in addition, modulation of voltage-operated calcium channels by NO has been demonstrated in several cell types, so it has been shown that NO modulates calcium influx through P/Q-type calcium channels in rat brain by inhibition of these channels (Petzold et al. 2005) and vice versa, activation of VOCCs by NO has been demostrated in other studies, for example, in rat sympathetic neurons (Chen and Schofield 1995).

1.11. Aim of the study

The present work aimed to investigate the action of the neurotransmitter nitric oxide on myenteric ganglia in the rat small intestine. The following questions should be answered:

- Does NO affect Ca^{2+} homeostasis in rat myenteric ganglia?
- Is this action mediated by Ca^{2+} channels in the cell membrane or mediated by intracellular stores of calcium?
- Which types of voltage-operated calcium channels are involved in this NO action?
- Which nitric oxide synthase isoforms are responsible for nitric oxide synthesis in myenteric ganglia?

2. Material and Methods

2.1. Animals

The experiments were carried out on five to twelve days old Wistar rats of both sexes. The rats were supplied by the Institute for Veterinary Physiology of the University of Gießen. The animals were kept in a housed room with a temperature of 22.5 °C, an air humidity of 50 – 55 %, and a 12 h :12 h light-dark cycle. The rats had access to water and standard diet ad libitum.

2.2. Solutions

2.2.1. Solutions for tissue preparation and cell culture

The isolation of the muscle layer containing the myenteric plexus was carried out in N-(2-hydroxyethyl)-piperazine-N´-(2-ethanolsulfonic acid) (= HEPES; 25 $mmol \cdot l^{-1}$)-buffered Dulbecco´s modified Eagle´s Medium (DMEM). Before use, the medium was supplemented with L-glutamine (final concentration: 4 $mmol \cdot l^{-1}$), gentamycin (final concentration: 20 $mg \cdot l^{-1}$), and metronidazol (final concentration: 5 $mg \cdot l^{-1}$). For the dissociation of the myenteric ganglia from the tunica muscularis, the tissue was incubated with the enzyme collagenase type 2 (268 - 273 $units \cdot mg^{-1}$), which was dissolved in DMEM (final collagenase concentration 1 $mg \cdot ml^{-1}$).

The obtained ganglia were incubated for one to three days in Start-V® medium (Biochrom AG, Berlin, Germany), a neuron specific medium,

supplemented with fetal calf serum (FCS; 10 % v/v). The medium was supplemented with the antibiotics penicillin G (100,000 units·l^{-1}) and streptomycin (100 mg·l^{-1}). In some experiments, the proinflammatory cytokine TNF-α (Tumor necrosis factor-α) was added to the cell culture medium in a concentration of 100 ng·ml^{-1}. For this purpose, TNF-α (1 µg) was dissolved in a stock solution of 1 ml autoclaved aqua dest with 1 mg bovine serum albumin (BSA).

2.2.2. Solutions for the fura-2 experiments

For the superfusion of the myenteric ganglia during the imaging experiments, a standard Tyrode solution was used containing (in mmol·l^{-1}): NaCl 140, KCl 5.4, HEPES 10, $CaCl_2$ 1.25, $MgCl_2$ 1, glucose 12.2. The pH of this solution was adjusted to 7.4 with NaOH/HCl. For the Ca^{2+}-freeTyrode solution, $CaCl_2$ was omitted.

2.2.3. Solutions for immunohistochemistry

The standard solution for these experiments was a phosphate-buffered saline (PBS) containing (in mmol·l^{-1}) NaCl 130, Na_2HPO_4 8, NaH_2PO_4 1.2. The pH was adjusted to 7.4 with NaOH/HCl. This solution was needed to wash the ganglionic preparation during the experiments from the remaining fixation solution and from the antibody-containing solutions. It was also used as the basic solution to prepare the blocking and the antibody-containing solutions. In addition, a 360 mmol·l^{-1}

phosphate buffer (PB) containing (in $mmol \cdot l^{-1}$) Na_2HPO_4 282 and NaH_2PO_4 76 was used as a stock solution for preparation of paraformaldehyde solution (PFA). Paraformaldehyde (4 %, w/v), diluted in 135 $mmol \cdot l^{-1}$ phosphate buffer, was used for the fixation of the myenteric ganglia. To prepare this solution, an equivalent amount of PFA (40 g) was weighted under the lab bench and dissolved in 1 l aqua dest. at 60 °C by permanent stirring and addition of NaOH. This solution had to be clear before it could be diluted with phosphate buffer up to a final concentration of 150 $mmol \cdot l^{-1}$. pH was adjusted to 7.4 with NaOH/HCl.

To permeabilize the cells and block unspecific binding sites, a Triton-X-containing phoshate-buffered saline (PBS-T) with 0.05 % (v/v) Triton-X was used, which was supplemented with 10 % (v/v) FCS.

2.3. Tissue preparation and cell culture

2.3.1. Tissue preparation

The rats were decapitated by a scissor (approved by Regierungspräsidium Gießen). The animals were fixed on a plate with needles through the foots, and the abdominal cavity was opened through a midline incision. All following steps were performed under a binocular microscope (Olympus SZX9; Olympus, Hamburg, Germany).

In order to remove the small intestine, the gut was cut off at the end of the rectum with a small scissor and carefully pulled out by a forceps, without injuring the bowel, until 5 cm distal to the pylorus of the stomach

and then cut off. Then the intestine was cleaned from the connective tissue by cutting away the mesentery as close as possible to the gut (Schäfer et al. 1997). The small intestine was separated from the colon through a cut proximal to the junction of the caecum.

The obtained gut preparation was transferred to a petridish of 35 mm diameter containing the preparation medium (DMEM). The muscle layer with adherent myenteric plexus was isolated from the mucosa by using two fine forceps (Dumont Nr. 5; Plano, Wetzlar, Germany). While fixing one end of the gut with one forceps, the muscularis was carefully pulled-away (“stripped”, similar as removing a stocking from a leg) until the end of the small intestine.

The obtained tissue was transferred to a 1.5 ml tube (Eppendorf, Hamburg, Germany) containing 500 µl DMEM and 500 µl collagenase stock solution (see above). It was incubated at 37 °C in a humidified atmosphere of 95 % O_2 and 5 % CO_2 (v/v) for enzymatic digesion for 2 h. After that time, the tube was vortexed for 30 s. The content of the Eppendorf tupe was gradually screened in a dish with DMEM under the microscope. Depending on the age of the animal used, some ganglia, forming net-like structures, could already be separated from the tunica muscularis at this stage of the praparation. By using a 20 µl pipette, the ganglia were collected and placed in a dish with DMEM on ice.

The partially digested muscle pieces were again transferred into a fresh collagenase solution and incubated for a further 2 h period. This

process could be repeated up to 4 times, however, by reducing the exposure time of the collagenase to periods of 30–60 min. Finally the isolated ganglia were transferred with a pipette into an autoclaved Eppendorf tube and centrifuged at 600 rpm for 10 min.

2.3.2. Culture of myenteric ganglia

All following steps were performed at the flow bench. For the culture of the myenteric gangila, conventional four-well-chamber (Nunc, Wiesbaden, Germany) and poly-L-lysine-coated glass coverslips (see below) were needed. First the supernatant was carefully sucked away with a pipette, and the pellet was re-suspended into Start-V® medium supplemented with 10 % (v/v) FCS. After passing the cell suspension a few times through the pipette to separate the myenteric ganglia into smaller pieces, the cells were transferred (50 µl for each well) into the culture chamber with the coverslips and incubated at 37 °C for 1 h to let the cells settle down on the coverslips. When the complete dissociation of the cells was desired, the cell suspension was passed through a needle (0.4 mm diameter). Finally the Start-V® volume in each well was completed to 500 µl. The chamber was replaced into the incubator; the cultured ganglia could be used for the experiment the next day.

2.3.3. Coverslips coating

For coating the coverslips, poly-L-lysine (molecular weight $>$ 300,000 D)

was used. The round cover glasses (13 mm; Nunc, Wiesbaden, Germany) were placed in 70 % (v/v) isopropyl alcohol at least two h to prevent a contamination of the preparation. Then they were washed thoroughly with autoclaved aqua dest. and transferred to a light protected tube (50 ml, Nunc GmbH, Wiesbaden, Gemany) with poly-L-lysine (0.1 $mg \cdot ml^{-1}$) diluted 1 : 5 in aqua dest. The coverslips were shaken on a shaker for about 3 h. Subsequently, the coverslips were carefully washed with aqua dest. and dried under light protection.

2.4. Imaging experiments

2.4.1. Principles of the method

In order to measure the cytosolic free Ca^{2+} concentration $[Ca^{2+}]_i$, a microscopic imaging technique was used based on the Ca^{2+}-sensitive indicator dye, fura-2. Fura-2 is the most popular Ca^{2+} indicator for microscopy of individual cells (Tsien 1989). Compared to the previous widely used dye, quin-2, fura-2 exhibits stronger changes in wavelength upon binding of Ca^{2+}, a higher selectivity for Ca^{2+} over other divalent cations, and it bleaches much less quickly than quin-2 (Grynkiewicz et al. 1985). Fura-2 belongs to the ratio indicator dyes or wavelength shifting dyes, which after complexing Ca^{2+} change either excitation or emission wavelength. Fura-2 binds Ca^{2+} with shifting its excitation spectrum from a wavelength of 360 nm to a wavelength of 340 nm (Figure 2.1).

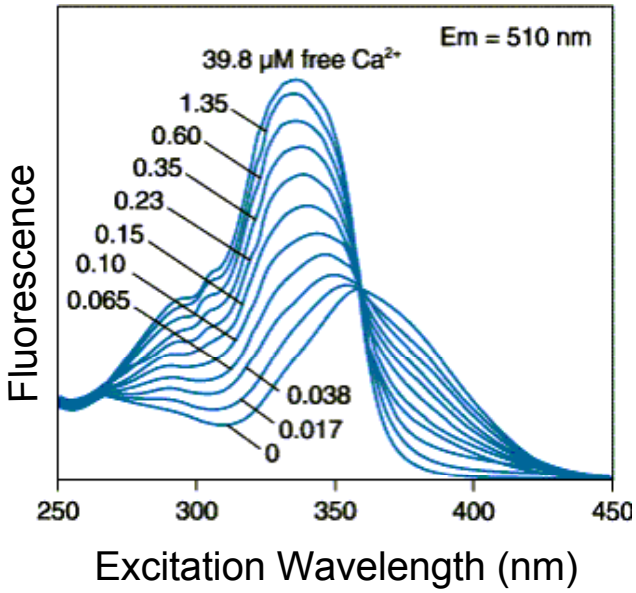

Figure 2.1: Excitation wavelengths of fura-2 at different free Ca^{2+} concentrations. Em = Emission wavelength.
From: www.probes.invitrogen.com/handbook/figures/0554.htm.

Consequently, both the free and the bound forms of the dye fluorescence strongly, so that they can be used for a ratio measurement, that means the alteration of the excitation wavelength between the two prefered wavelengths permits the measurement of the ratio of the Ca^{2+} bound dye and the free dye. From this value, the cytosolic Ca^{2+} concentration can be calculated (Tsien et al. 1985).

The green emission from fura-2 peaks at 505 – 520 nm and does not shift significantly after Ca^{2+} binding. The two preferred excitation wavelengths were 340 nm and 380 nm, where the ratio signal shows the largest dynamic range (Tsien 1989). This ratio method cancels out the effects of many factors that can appear during measurement at single wavelength as with quin-2, i.e. the fluorescence intensity from

excitation at single wavelength is dependent on the dye concentration, the cell thickness, and instrumental factors such as lamp intensity. The dye concentration varies from cell to cell and decreases gradually due to bleaching and leakage, the thickness of cells varies from cell to cell and from position to position within a cell, and the illumination intensity varies over the field of view of a microscope. The ratio operation cancels out these uncertainties by measuring the shape or wavelength distribution of the fluorescence spectrum rather than its absolute amplitude (Tsien et al.1985).

From the ratio signal, the cytosolic Ca^{2+} concentration can be calculated using the so-called Grynkiewicz equation (Grynkiewicz et al.1985).

$$[Ca^{2+}]_i = \frac{K_D * \beta * (R - R_{min})}{(R - R_{max})}$$

Where:

K_D = dissociation constant

ß = fluorescence during excitation at 340 nm (at 0 $\mu mol \cdot l^{-1}$ Ca^{2+}) divided by the fluorescence during excitation at 380 nm (at 39.8 $\mu mol \cdot l^{-1}$ Ca^{2+})

R = measured ratio

R_{min} ,R_{max} = ratio at 0 and 39.8 $\mu mol \cdot l^{-1}$ Ca^{2+}, respectively.

Fura-2 has a high selectivity for Ca^{2+} over Mg^{2+} and other divalent cations. It is only poorly affected by intracellular pH changes. It is derived from the parent compound 1,2-bis(O-aminophenoxy)ethane-N,N,N',N'-tetraacetic acid (BAPTA), which is a derivative of the Ca^{2+} chelator EGTA (ethylene-glycol-bis(β-aminoethyl ether)-N,N,N',N'-tetraacetic acid), to which refers the good discrimination between Mg^{2+}/Ca^{2+} of the fura-2, i.e, the binding cavity has the right size for Ca^{2+} but can not envelope Mg^{2+}, because the carboxylates at each end of the chain will butt into each other (Tsien 1980) (Figure 2.2).

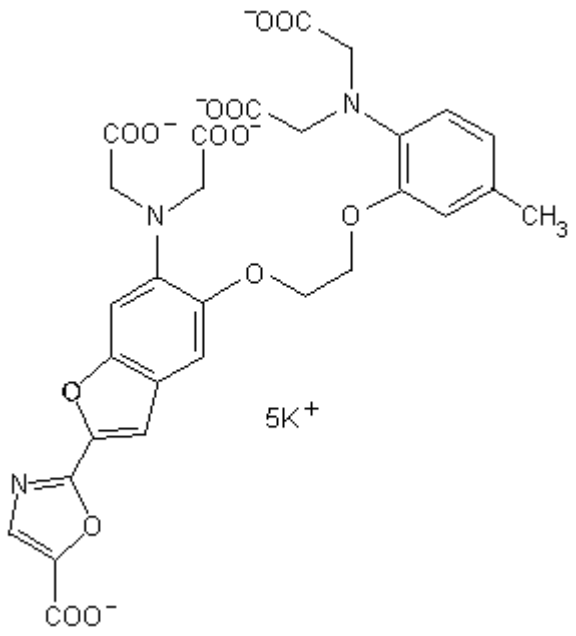

Figure 2.2: Structure of fura-2. From: www-user.tu-chemnitz.de/awill/diplom/fura2.htm.

Monovalent cations do not form detectable complexes, probably because their charge is inadequate to bind the negative carboxylates (Tsien 1989). Fura-2 has a dissociation constant for Ca^{2+} of approximately 224 $nmol \cdot l^{-1}$ and can be used to measure intracellular Ca^{2+} concentrations ranging from about 2.24 to 22400 $nmol \cdot l^{-1}$. The dissociation constant is defined as the value, at which 50 % of the fluorescent dye has bound the target ion. This low affinity for Ca^{2+} permits measure of high $[Ca^{2+}]_i$ values up to several micromolar (Tsien et al. 1985). Since the basal cytosolic Ca^{2+} averages in general 100 $nmol \cdot l^{-1}$, fura-2 can encompass the increase in $[Ca^{2+}]_i$ under most physiologic situations.

Fura-2 is a charged molecule which can not permeate the intact cell membrane. Therefore, for loading the cells, the liphophilic fura-2-acetoxymethylester (fura-2/AM) was used, in which the four carboxylate groups are masked with ester groups. Inside the cell, the ester groups are hydrolysed through nonspecific esterases and the orginal chelator is trapped in the cytosol (Tsien 1981).

The accurate calculation of intracellular Ca^{2+} concentration by the Grynkiewicz equation (see above) is not absolutely reliable, since the fluorescence signal is influenced by many intracellular factors such intracellular proteins or osmolarity (Baylor et al. 2000). Therefore, in this work (as it is meanwhile standard for most studies using fura-2), only

changes in the fura-2 signal ratio as indicator for $[Ca^{2+}]_i$ are given.

2.4.2. The experimental setup

An inverted light microscope was used (Olympus IX-50, Olympus, Hamburg, Germany), equipped with an epifluorescence setup and an imaging analyse software (Till Photonics, Martinsried, Germany). A monochromator is the central unit of the system. The light from an integrated xenon light source, which is adjusted to the desired wavelengths with the help of a control unit of the monochromator and the imaging software, is collected through lenses and mirrors to generate the desired excitation wavelength. The excitation light is focused onto the lightguide of the monochromator. The monochromatic light is linked to the microscope via an epifluorescence condensor. A dichroic mirror receives the excitation light and reflects it through the microscope objective to the cells. The emitted light from the cells passes the mirror across an emission filter, then it is received from a charge-coupled device (CCD) camera and converted into digitized images. The camera is connected to a frame grabber in the computer. In the computer, the image data are processed before they are displayed on the screen during the so-called live mode of the imaging software (Figure 2.3).

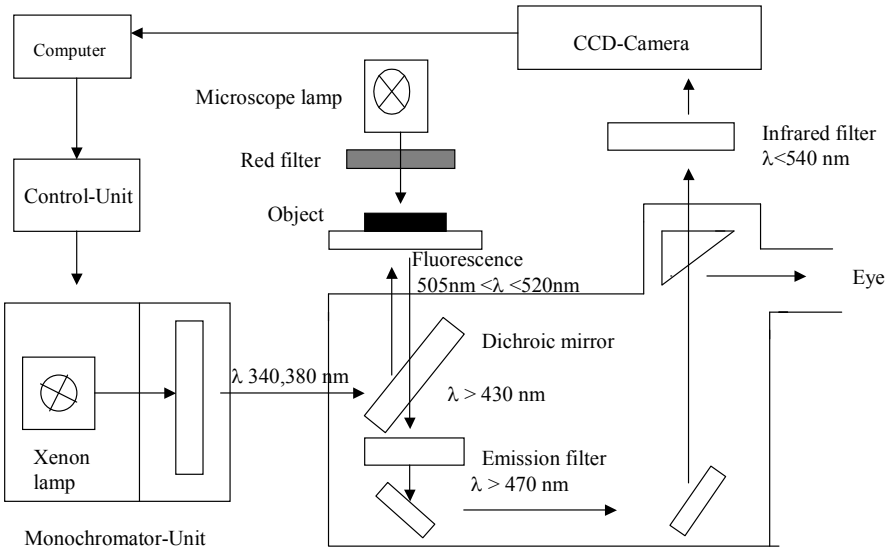

Figure 2.3: Schematic of the imaging apparatus

2.4.3. Experimental procedure

The cells were loaded with fura-2/AM (6 µl, 5 $\mu mol \cdot l^{-1}$ final concentration) in DMEM (total volume: 500 µl) with pluronic acid (0.05 % (w/v) final concentration) for 60 min at room temperature. Pluronic acid is a detergent; it was used to improve the solubility of fura-2/AM. This process was achieved in the experimental chamber and in darkness, because of the sensitivity of fura-2 to light. After rinsing the cells three times with fresh DMEM, the coverslip with the attached cells was fixed by screws over a hole in the bottom of a selfcreated chamber with a

volume of 3 ml. The chamber was transferred to the stage of the microscope. After perfusing the cells with Tyrode solution to remove the DMEM, a suitable field of cells was chosen for the measurement. After the connection of the microscope to the camera and start of the software, several cells whithin the image analysis software were chosen (region of interest) and marked. Now the recording of the image could begin by alternative exposure of the cells to the selected excitation wavelength (340 nm and 380 nm) at an emission wavelength of 510 nm. The exposure time was 20 ms for each excitation wavelength. This was repeated every 5 s (sampling rate 0.2 Hz). Baseline fluorescence was recorded at the beginning of the experiment (superfusion with Tyrode solution for a few minutes), then the subsequent $[Ca^{2+}]_i$ changes upon drug administration were determined.

An infusion set was used to superfuse the preparation hydrostatically (perfusion rate about 1 $ml \cdot min^{-1}$) throughout the experiment.

2.5. Polymerase chain reaction (PCR)

Polymerase chain reaction was developed by Kary B. Mullis in 1985 (Mullis was a scientist for the Cetus corporation in California), he awarded the Nobel prize in chemistry in 1993 for his discovery of the PCR method (Newton and Graham 1997).

2.5.1. Basic principles of PCR

PCR is a technique for amplifying specific DNA sequences (targets) that is currently used in a wide variety of molecular biology applications (Mullis and Faloona 1987).The amplifying of a DNA sequence (double stranded) is performed in three steps. In the denaturing step, the DNA sequence is separated through application of a high temperature to about 95 °C into two single strands termed templates, which are in the annealing step hybridized with a short single stranded DNA molecule called primer. The primer must to be long enough (18 to 24 nucleotides) to reduce the probability of the sequence binding at non target sites (Saiki et al. 1985). Two different primers bind after cooling down the reaction mixture to about 50 - 65°C, a sense (or forward) and an anti-sense (or backward) primer. Only the template molecules that have a sequence complementary to the primer will recognize and bind the DNA polymerase. The last step is the polymerization reaction, an extension of the primer-template molecule at 72 °C through the thermostable (Taq) DNA polymerase (a frequently used enzyme isolated from the heat stable bacterium, Thermus aquaticus) by binding a complementary nucleotide to each nucleotide in the template strand in the presence of deoxynucleotides triphosphates (dNTPs, i.e. a mixture of dATP, dTTP, dGTP, dCTP) and magnesium chlorid, in the direction from the primer to the other end. The cycle of three steps is repeated 30 - 50 times and the

DNA molecules that were synthesized in a cycle are used as templates in the following one (Stolovitzky and Cechi 1996) (Figure 2.4).

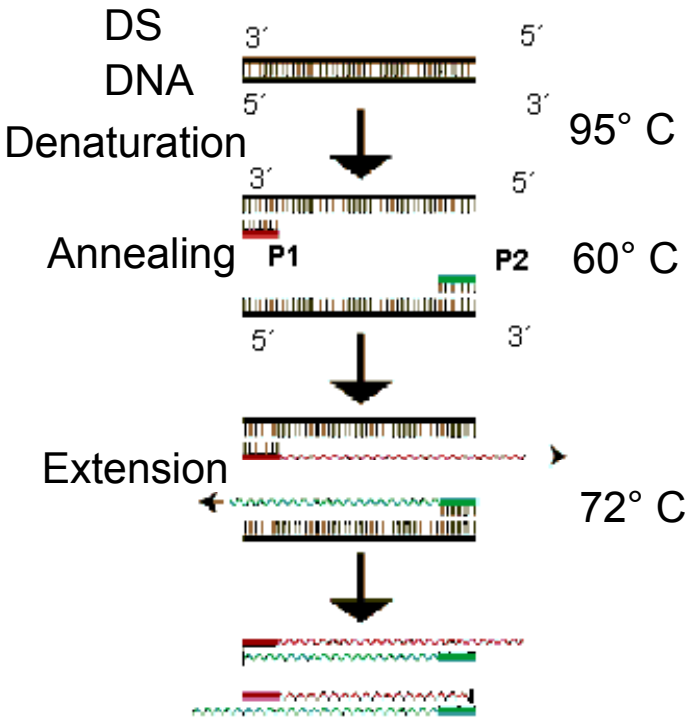

Figure 2.4: Polymerase chain reaction. DS-DNA = double-stranded DNA; P = Primer (from www.flmnh.ufl.edu/cowries/PCR).

2.5.2. Gel electrophoresis of DNA

Electrophoresis through an agarose gel is the standard method to separate, identify and purify DNA fragments (Sharp et al. 1973). Applying an electric field across the gel lets the DNA, which is negatively charged at neutral pH, migrate toward the positive electrode. The location of the DNA within the gel can be controlled directly by staining the sample with a low concentration of the fluorescent dye,

ethidium bromide, which intercalates between base pairs of the DNA. Bands containing as little as 1 – 10 ng of DNA can be detected by exposure of the stained gel to the ultraviolet light. TAE (Tris-acetate/EDTA buffer; composition see below) is the most commonly used buffer. The electrophoretic mobility of DNA is affected by the composition and the ionic strength of the electrophoresis buffer, in the absence of buffer the electrical conductance is minimal and DNA migrates slowly. It is important to use the same batch of electrophoresis buffer in both the electrophoresis tank and the gel, as small differences in ionic strength can greatly affect the motility of DNA fragments (Sambrook et al. 1989).

2.5.3. Experimental procedure

The experiment should be performed under sterile conditions to prevent microbial contamination which can be a source of RNAse .

RNA extraction

For eNOS and iNOS isoform determination, the total RNA was extracted from samples using a commercial kit (Rneasy kit, Qiagen, Heiden, Germany).

1. Lysis of the cells

First the cells were centrifuged at 600 rpm for 10 min. Subsequently, the supernatant was removed, the pellet was resuspended in 600 µl lysis buffer (RTL-buffer from the Rneasy kit) with β-mercaptoethanol (1% (v/v)). Because the latter product is toxic, this step had to be performed under the lab blech. By applying a thorough vortexing, the cell lysate was completely homogenized.

2. Isolation of RNA

700 µl of the homogenized sample was transferred into a Qia shreder tube (provided with the kit) and centrifuged at 1500 rpm for 2 min. The lysate in the lower part of the tube was sealed (with cover provided with the kit) and centrifuged for 3 min at 1500 rpm. The supernatant was transferred to a new tube (Eppendorf, Hamburg, Germany) followed by adding the same volume of ethanol (70 % (v/v)) and thoroughly vortexing. 700 µl of the sample was pipetted to Rneasy-Mini spin column (provided by the kit) and centrifuged for 45 s at 1500 rpm. The supernatant was removed and 700 µl RW1 buffer (provided with the kit) was added to a spin column and centrifuged for 45 s at 1500 rpm. After the tube with the supernatant was removed, the spin column was placed on a new 2 ml tube and 500 µl RPE buffer (provided with the kit; diluted in 96-100 % (v/v) ethanol, 200 µl/800 µl respectively) was added followed by 45 s centrifugation at 1500 rpm. RW1 and RPE are used for

elution of RNA under low-salt condition. This step was repeated by adding 500 µl diluted RPE buffer after the supernatant was sucked away and centrifugation for 2 min. The supernatant was removed. The spin column was pulled carefully out from the lower tube and placed on a new 1.5 ml tube followed by adding 30–50 µl RNAse free DEPC-water (diethylpyrocarbonate; 1 ml DEPC/l Aqua dest) and centrifugation for 1 min at 8000 rpm. The supernatant with the prepared RNA can be stored at –20 °C.

3. Isolation of mRNA (poly A^+-RNA)

The isolation of mRNA from the total RNA was carried out through binding of mRNA to oligotex-resin in OBB-buffer (provided with the kit) under high salt condition and the elution in OEB-buffer (provided with the kit) under low salt condition using OligoTex® Qiagen.

The Oligotex-suspension and the OEB-buffer were being warmed at 37 °C and 70 °C, respectively in a heating block. 250 µl RNAse free water was added to the total RNA sample tube followed by adding 250 µl OBB-buffer and 15 µl of warmed Oligotex-Suspension. The mixture was thoroughly vortexed and incubated for 3 min at 70 °C in a heating block. After cooling of the mixture for 10 min at room temperature (hybridisation of mRNA to the OligoT30-Nucleotide in Oligotex-resin), the tube was centrifuged for 2 min at 15,000 rpm and the supernatant

was carefully removed. Following resuspension of the Oligotex-mRNA-pellet in 400 µl OW2-buffer and strong vortexing, the suspension was transferred to a small spin column placed on a 1.5 ml tube and centrifuged for 1 min at 15,000 rpm. The tube with the supernatant was removed and the spin column was placed on a new tube. After adding 400 µl OW2-buffer, the last step was repeated. The spin column was placed on a new tube, 20 µl from prewarmed OEB-bufffer was added and a repetitive pipetting applied to resolve the resin from the column in the buffer suspension. The tube was centrifuged at 15,000 rpm for 1 min followed by adding 20 µl of warmed OEB-buffer and the last step was repeated. After centrifugation, the spin column was removed, and the mRNA in the supernatant could be used in RT-PCR.

Reverse transcriptase reaction

Using cMaster RT-kit (Eppendorf, Hamburg, Germany) cDNA was reverse transcribed from poly A^+-RNA in a reaction mixture of 20 µl. All substances of cMaster kit had to be placed on ice and centrifuged before use by the mean of a table-top centrifuge (Qualitron Dw-41).

The procedure

The constituents of the cMaster kit were pipetted in a sterile tube as followed: 3.5 µl RNase free water, 4 µl RTplus buffer (25 $mmol \cdot l^{-1}$ Mg^{2+}), 2 µl dNTPs (10 $mmol \cdot l^{-1}$), 2 µl cMasterRt enzyme, 0.5 µl primer RNAse

inhibitor (provided with the cMaster kit). In another tube were transferred: 6 µl poly A^+-RNA and 2 µl Oligo dT Primer (Promega C110A), they were incubated for 5 min at 65 °C to resolve the base pairs in single strands. The tube was immediately placed on ice. After adding of the 12 µl mastermix, the reaction mixture was transferred to a thermocycler and run at 42 °C for 60 min.

The resultant of the reverse transcriptase reaction, the cDNA, was immediately diluted (1:10) in DNase-RNase-free water (Sigma, Taufkirchen, Germany) and determined using a spectrophotometer at $\lambda = 260$ nm. The cDNA could be stored at -20°C.

Isolation of RNA of the nNOS isoform

The total RNA was extracted from cell samples using Trizol reagent (Invitrogen, Karlsruhe, Germany) according to the manufacturer's instructions. Isolation of RNA by means of this reagent is an improvement to the single-step RNA isolation, wich is free of protein and DNA contamination.

The procedure

1. Homogenization

The cells were pelleted by centrifugation and lysed in 1 ml Trizol reagent. The cell lysate was completely homogenized by passing it several times through a pipette.

2. Phase separation

The homogenized sample was incubated for 5 min at room temperature. Then 200 µl of chloroform was added. The tube was thoroughly shaken for 15 s and incubated at room temperature for 2 min. The sample was centrifuged at 12,000 rpm for 15 min at 4 °C. Following centrifugation, the mixture was separated into three layers, a lower, a middle and a colorless upper aqueous layer. RNA is exclusively found in the upper layer.

3. RNA precipitation

The aqueous phase was transferred into a new tube. 500 µl of isopropyl alcohol was added to precipitate the RNA. The sample was incubated at room temperature for 10 min and centrifuged at 12,000 rpm for 10 min at 4 °C.

4. RNA wash

The supernatant was removed and RNA was washed with 1 ml 75 % (v/v) ethanol. The sample was mixed by vortexing and centrifuged at 7,500 rpm for 5 min at 4 °C.

5. Redissolving the RNA

The RNA pellet was partially dried by air-drying for 5 - 10 min and dissolved in 30–50 µl RNase free water by passing the solution a few

times through the pipette tip. The RNA sample was incubated at 55 to 60°C for 10 min. This RNA was used in reverse transcriptase reaction as described above.

2.5.4. The PCR reaction

cDNA was amplified by using Eppendorf Master mix (2.5 x) in a total volume of 25 µl with 1.25 U Taq DNA polymerase, 200 $\mu mol \cdot l^{-1}$ dNTPs mixture, and $MgCl_2$ (1.5 $mmol \cdot l^{-1}$ or 2.5 $mmol \cdot l^{-1}$ or 3.5 $mmol \cdot l^{-1}$). Sense and antisense primer were used against rat eNOS, nNOS, iNOS (Schricker et al. 1996) and GAPDH (a constitutively expressed gene used as a control for the efficiency of cDNA synthesis). They were obained from MWG Biotech (Ebersberg,Germany) and are listed in Table 2.1.

The PCR amplification protocol was as follows: 10 min at 94 °C, 40 cycles with 1 min of denaturation at 94 °C, 1 min of annealing at 60 °C and 2 min of extension at 72 °C followed by a final elongation for 10 min at 72°C on a thermal cycler (Eppendorf, Hamburg, Germany). The amplified products were electrophoresed on 1.5 % agarose gel.

Table 2.1. Sequences of sense and antisense primers of rat eNOS, nNOS, iNOS, and GAPDH.

Target molecule	Accession code	Sence primer	Antisense primer
eNOS	NM 000603	5′ - CTG CTG CCC GAG ATA TCT TC- 3′	5′ - AAG TAA GTG AGA GAG CCT GGC GCA- 3′
nNOS	NM 052799	5′-GAA TAC CAG CCT GAT CCA -3′	5′-TCC AGG AGG GTG TCC ACC GCA-3′
iNOS	NM 012611	5′-GCA GCT GTG CTC CAT AGT-3′	5′-GAT AGG ACG TAG TTC AAC AT-3′
GAPDH	BC 059110	5′-ACG GGA AGC TCA CTG GCA TG- 3′	5′-CCA CCA CCC TGT TGC TGT AG-3′

2.5.5. Electrophoresis of the PCR products

A 1.5 % (w/v) agarose gel was prepared by adding 100 ml 1x TAE buffer (Tris-acetate/EDTA; Molecular Probes, Ohio, USA) which consisted of Tris acetate 40 $mmol \cdot l^{-1}$, EDTA 1 $mmol \cdot l^{-1}$, pH 8.15) to 1.5 g agarose (peqlab, Erlangen, Germany). The mixture was heated and boiled until the agarose was dissolved and the suspension appeared clear. While the agarose cooled down, the electrophoresis apparatus

was installed by sealing the edges of the plastic plate with rubber bands and setting into the electrophoresis tank. The comb was positioned 0.5 mm above the plate, so that a complete well was formed when the agarose was added. After removing the gel layer above, the agarose was poured into the mold. Bubbles within the gel and under the teeth of the comb had to be avoided.

After the gel was set, the comb and the rubber were carefully removed and 1 x TAE buffer was added to a level of about 0.5 cm above the gel. After the DNA samples were mixed with 2 µl loading dye, they were pippeted (using a 10 µl pipette) into the slots and 5 µl of 50 bp-ladder was loaded into the first and the last slots. The lid of the electrophoresis tank was closed. The voltage supply was attached and the electrophoresis was run for 2.5 h. After the run, the electric current was turned off, the lid was removed and the gel was carefully transferred to stain with ethidium bromide.

2.5.6. Visualization of DNA in agarose gel

The amplified products were visualized by staining the gel through immersion in aqua dest. containing the fluorescent dye ethidium bromide (1 $mg \cdot l^{-1}$) for 10 min. The ethidium bromide not bound to DNA was removed by soaking the stained gel in water for 10 min. The DNA bands were visualized, photographed by exposing the gel to ultraviolet

light (302 nm) and quantified using an image analyzing software (Bio Capt; Vilber Lourmat, Marge-La-Vallée, France).

2.6. Immunohistochemical experiments

2.6.1. Principles of the method

Immunohistochemistry is the in situ-detection of antigens in tissue sections and cells by specific monoclonal or polyclonal antibodies. Detection is obtained by visualization of antigens by a light microscopy-detectable fluorochrome conjugated to the antibody. Immunohistochemistry enables visualization of the distribution and localization of specific cellular components within a cell or tissue.The most widely used methods of detection work with enzyme-antibody conjugates such as peroxidases or fluorophore-antibody labeled with fluorescent dyes such as Alexa-fluor.

The antibodies used can be polyclonal or monoclonal. Polyclonal antibodies are antibodies isolated from whole serum after a secondary immune response has been stimulated by injecting an antigen in an animal. They are a heterogenous mixture of antibodies that recognize several epitopes of antigens, but the disadvantage of this type is that they may cause unspecific background fluorescence. Monoclonal antibodies, however, are isolated from specific immunocytes (plasma cells) after stimulation of a secondary immune response. These cells are cultured, if the cells are genetically identical, they produce

monoclonal antibodies, which exhibit greater specificity (Noll and Schaub-Kuhnen 2000).

There are two strategies used for the immunohistochemical detection of antigens in a tissue, the direct and the indirect method. In the direct method, a labeled antibody reacts directly with the antigen in cells. This method is rapid and simple, but has the disadvantage that it depends on the production of labeled antibodies against every antigen of interest. For the indirect fluorescence, however, a secondary antibody conjugated with a marker is used to visualize the antigen-antibody complex. The secondary antibody must be directed against the immunoglobuline of the animal species in which the primary antibody has been raised. This method has a higher sensitivity compared to the direct approach, because there can be several reactions sites on the primary antibody, which react with the secondary antibody and produce a good signal. Another advantage of the indirect technique is that there is no need to generate specific secondary antibody for every primary antibody, so a secondary antibody raised against IgG of a certain species can be used with any primary antibody raised in this animal (Larsson 1988).

I have determined NOS isoforms (nNOS, eNOS, iNOS) by using the indirect method in dissociated cells attached to coated coverslips. The determination of NOS isoforms in some experiments was combined with the differentiation between glia and neurons in the same preparation

using double labelling technique. So mouse monoclonal anti-PGP 9.5 (protein gene product 9.5; Dianova, Hamburg, Germany) was used for labelling of the neurons. Mouse monoclonal anti-GFAP (glial fibrillary acidic protein; Chemicon, Hofheim, Germany) was used for labelling of glial cells. As secondary antibodies for both primary antibodies, Alexa-conjugated goat anti-mouse polyclonal Alexa Flour®488 (Invitrogen, Karlsruhe, Germany) was used. For investigation of NOS isoforms, rabbit anti-bNOS (Becton Dickinson, Heidelberg, Germany), rabbit anti-eNOS (Chemicon, Hofheim, Germany), rabbit anti-iNOS (Chemicon, Hofheim, Germany) and the secondary Cy3-conjugated donkey anti rabbit were used (Table 2.2).

2.6.2. Experimental procedure

The experiments were carried out in the culture chambers and at room temperature. The volume of the solution for rinsing and incubation of the preparation was 500 µl. After the incubation medium was sucked away, the preparation was washed 3 times for 2 min with PBS. The cells were fixed with freshly prepared 4 % (w/v) PFA solution for 15 min. The preparation was washed 3 times with PBS for 2 min. The cells were permeabilized and nonspecific sites were blocked by incubation of the preparation with 10 % (v/v) FCS in 0.05 % (v/v) Triton X-100/PBS for 60 min. Subsequently, the cells were incubated with primary antibodies diluted in FCS-Triton/PBS at 4°C for 48 h.

Table 2.2: Primary and secondary antibodies used in staining the cultured myenteric cells

Primary	Host	Dose	Secondary	Dose
nNOS	Rabbit	1:800	Donkey anti-rabbit CY3	1:800
eNOS	Rabbit	1:800	Donkey anti-rabbit CY3	1:800
iNOS	Rabbit	1:200	Donkey anti-rabbit CY3	1:800
PGP 9.5	Mouse	1:500	Goat anti-mouse Alexa fluor 488	1:500
GFAP	Mouse	1:500	Goat anti-mouse Alexa fluor 488	1:500

The negative control was performed by omitting the primary antibodies. After the cells were rinsed 3 times for 2 min with PBS-T, the incubation with secondary antibodies diluted in FCS-Triton/PBS (Cy3 conjugated donkey anti-rabbit, 1:800 and Alexa Flour goat anti-mouse, 1:500) for 2 h at room temperature and in darkness was performed. After a washing step the cells were stained with the nuclear dye DAPI (4´,6-Diamidino-2-phenylindol dilactat, 300 $nmol \cdot l^{-1}$) for 5 min followed by washing 3 times with PBS-T. The cells then were embedded using Citiflour® (glycerol-PB, Newby Castleman, Leicester, UK) on object slides and covered. The cells were observed and photographed with a light microscope (Eclipse 80i, Nikon, Düsseldorf, Germany) equipped with a digital camera (Digital Sight DS-2MBWc, Nikon, Düsseldorf, Germany). Images were only analyzed qualitatively and no quantification of NOS-positive cells was performed.

2.7. Chemicals

Fura-2/AM (Molecular Probes, Leiden, The Netherlands), and pluronic® (BASF, Weyandotte, USA) were dissolved as stock in dimethylsulfoxide (DMSO). GEA 3162 (Axxora, Grünberg, Germany), SNP (Calbiochem, Bad Soden, Germany), $NiCl_2$, $CoCl_2$, verapamil and carbachol were dissolved in Tyrode solution. Nifedipine was dissolved in ethanol (final concentration 0.02 %, v/v), ω-conotoxine GVIA and ω-agatoxin IVA (both from Alomone, Jerusalem, Israel) were dissolved in Tyrode solution containing $1 g \cdot l^{-1}$ BSA. DAPI (4´,6-diamidino-2-phenylindol dilactate) was dissolved as stock in Aqua dest (final concentration 300 $nmol \cdot l^{-1}$). If not indicated differently, drugs were obtained from Sigma (Taufkirchen, Germany).

2.8 Statistics

Results are given as means ± standard error of the mean (SEM) with the number (n) of investigated cells. For the comparison of two groups, either a Student's t-test or a Mann-Whitney U-test was applied. An F-test decided which test method had to be used. Both paired and unpaired two-tailed Student's t-tests were applied as appropriate. When the mean values of more than two groups had to be compared, an one-way ANOVA test was performed followed by analysis of linear contrasts with the test of Scheffé.

3. Results

3.1. Effect of NO donors on the intracellular Ca^{2+} concentration in the myenteric ganglia

After loading the myenteric ganglia with fura-2/AM, the lipophilic precursor of the Ca^{2+}-sensitive dye fura-2, the response of these cells to an NO-donor such as GEA 3162 or sodium nitroprusside (for references of the drugs, see Schultheiss et al. 2002) was tested. First, the fura-2 ratio signal was measured under baseline conditions, i.e during superfusion with Tyrode solution. Under these conditions, the fura-2 ratio amounted to 0.43 ± 0.013 (n = 66). Subsequently, GEA 3162 (10^{-4} $mol \cdot l^{-1}$) was administered. The NO donor induced a pronounced increase in the fura-2 ratio signal to 0.51 ± 0.018 ($p < 0.05$ versus baseline, n = 66; Figure 3.1, Table 3.1), indicating an increase in the cytosolic Ca^{2+} concentration.

At the end of all fura-2 experiments, cell viability was checked by administration of either carbachol ($5 \cdot 10^{-5}$ $mol \cdot l^{-1}$), a cholinergic agonist, or of cyclopiazonic acid (CPA; $5 \cdot 10^{-5}$ $mol \cdot l^{-1}$). Carbachol induces an increase in the cytosolic Ca^{2+} concentration via stimulation of nicotinic receptors (Rehn et al. 2004). Cyclopiazonic acid, however, acts as blocker of sarcoplasmic-endoplasmic reticulum Ca^{2+}-ATPases (SERCA), which causes an increase in the cytosolic Ca^{2+} concentration by inhibiting the uptake of Ca^{2+} into intracellular Ca^{2+} stores (Moncoq et

al. 2005). All cells responding to carbachol or CPA were included in the statistical analysis.

The effect of GEA 3162 was mimicked by another NO donor, sodium nitroprusside (Figure 3.2).

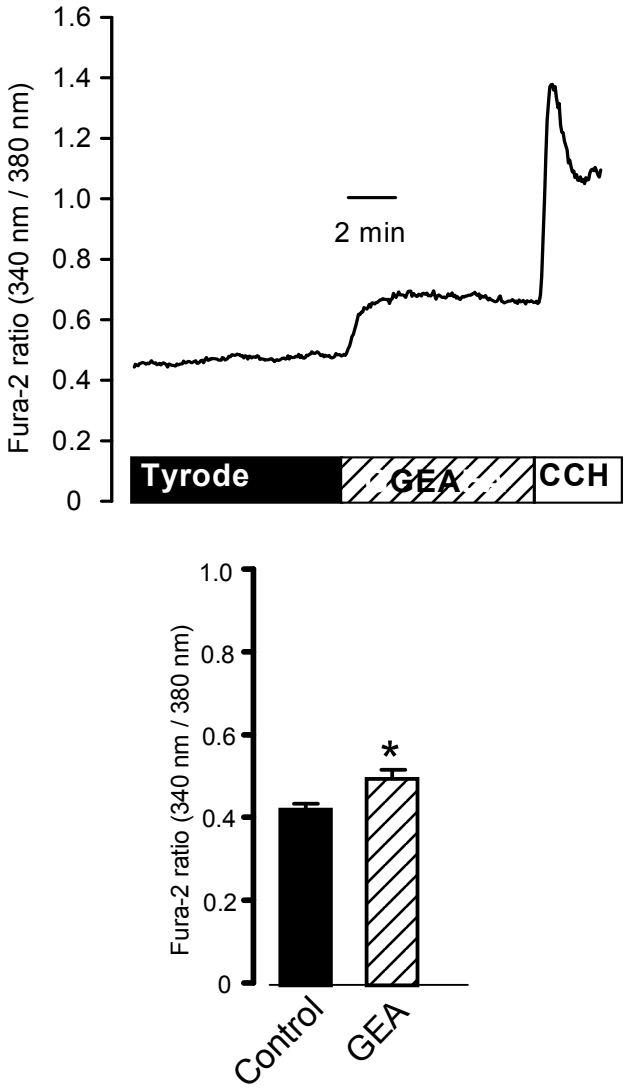

Figure 3.1: Administration of GEA 3162 (10^{-4} mol·l^{-1}) induced an increase in the fura-2 ratio at cultured myenteric ganglia as shown in an original record (top). In average (bottom), the fura-2 ratio increased from 0.43 ± 0.01 under control conditions (black bar) to 0.51 ± 0.02 in the presence of GEA 3162 (shaded bar; n = 66). Values are means ± S.E.M., * $p < 0.05$ versus control just prior administration of GEA 3162. Cell viability was confirmed at the end of each experiment by administation of carbachol (CCH; $5 \cdot 10^{-5}$ mol·l^{-1}).

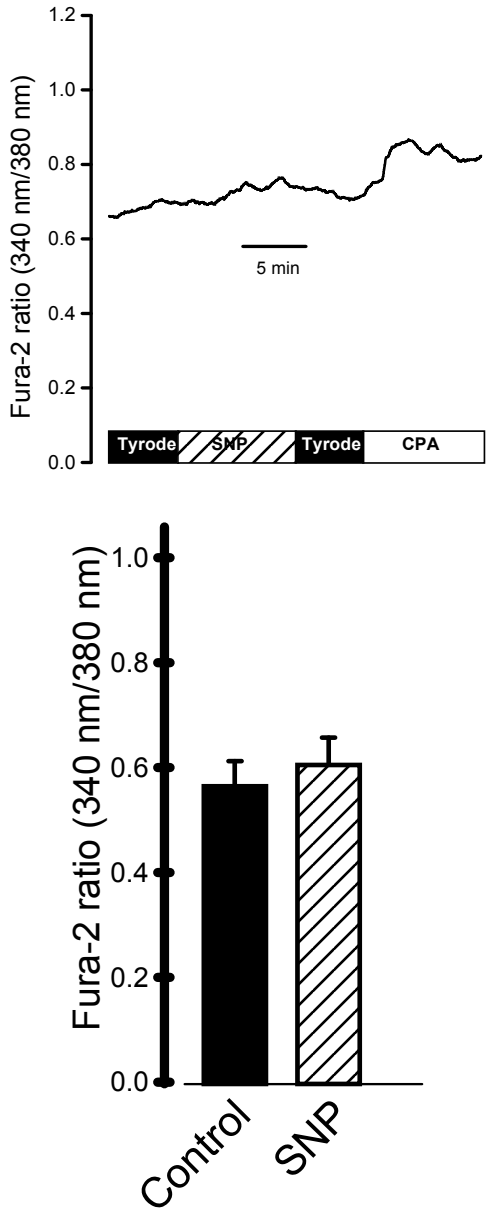

Figure 3.2: The NO donor, sodium nitroprusside (10^{-4} mol·l^{-1}; SNP) caused an increase in the fura-2 ratio at cultured myenteric ganglia as shown in an original record (top). In average (bottom), the fura-2 ratio signal increased from 0.56 ± 0.047 under control conditions (black bar) to 0.60 ± 0.051 in the presence of SNP (shaded bar; n = 19). Values are means ± S.E.M., $p < 0.05$ versus control just prior administration of SNP. Cell viability was confirmed at the end of each experiment by administation of the SERCA blocker, cyclopiazonic acid (CPA; $5 \cdot 10^{-5}$ mol·l^{-1}).

3.2. The effect of NO donors is dependent on the presence of extracellular Ca^{2+}

In the next series of experiments, it should be determined whether the increase in the intracllular Ca^{2+} concentration induced by the NO-donors was caused by a Ca^{2+} release from intracellular stores or by a Ca^{2+} influx from the extracellular space. Therefore, the ganglia were superfused with a Ca^{2+}-free Tyrode solution in order to prevent Ca^{2+} influx across the plasma membrane. All these experiments were performed with GEA 3162, the more potent of the two tested NO donors.

In the absence of extracellular Ca^{2+}, the action of the NO-donor on the fura-2 signal was completely suppressed (Figure 3.3). Cell viability was tested by administration of cyclopiazonic acid, which evoked an increase in the cytosolic Ca^{2+} concentration even in the absence of extracellular Ca^{2+} indicating that cell viability was preserved under these conditions.

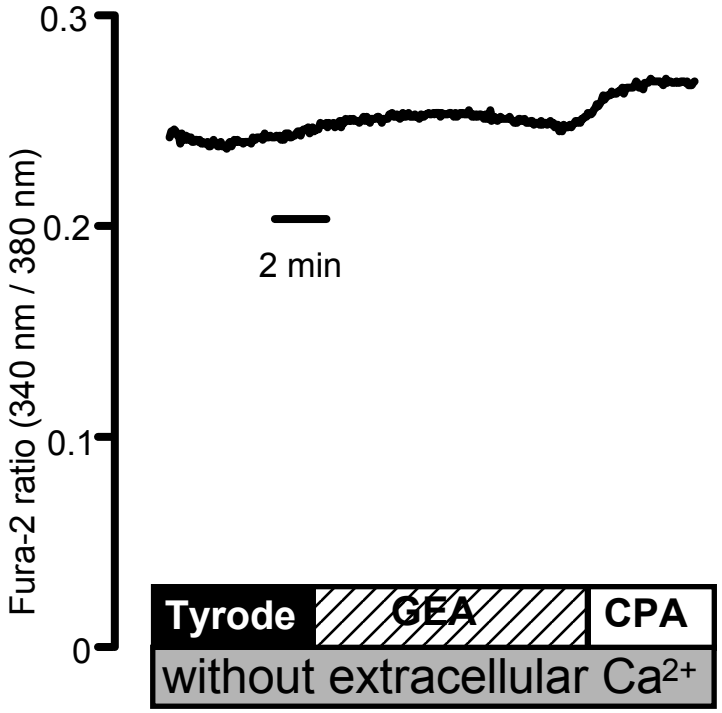

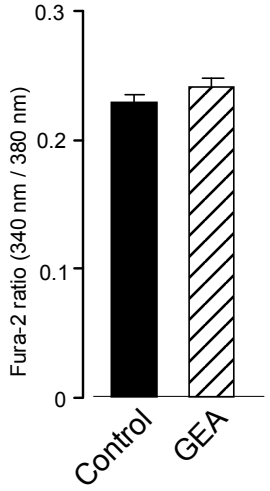

Figure 3.3: Effect of GEA 3162 (10^{-4} mol·l^{-1}) on the fura-2 ratio in the absence of extracelllular Ca^{2+} as shown in an original record (top). In average (bottom), GEA 3162 caused only a small, statistically insignificant increase of the fura-2 ratio from 0.23 ± 0.01 under control conditions (black bar) to 0.24 ± 0.01 in the presence of GEA 3162 (shaded bar; n = 42; p > 0.05 versus fura-2 ratio in the absence of GEA 3162). Values are means ± S.E.M. Cell viability was confirmed at the end of each experiment by administation of the SERCA blocker, cyclopiazonic acid (CPA; $5 \cdot 10^{-5}$ mol·l^{-1}).

3.3. Involvement of voltage-dependent Ca^{2+}channels

The predominant Ca^{2+} transporters, which are responsible for an influx of Ca^{2+} across the plasma membrane in excitable cells such as neurons are voltage-dependent Ca^{2+} channels (Catterall et al. 2003). In order to investigate the possible involvement of these ion channels in the NO response at rat myenteric ganglia, the ability of different blockers of voltage-dependent Ca^{2+} channels to interfere with the NO response was tested. All blockers were used in concentrations which were known to exert a maximal effect at rat myenteric ganglia (Schäufele and Diener 2005).

Many types of voltage-dependent Ca^{2+} channels can be inhibited by divalent cations such as Ni^{2+} and Co^{2+} (N'Gouemo and Morad 2003). Pretreatment of the ganglia with Ni^{2+} ($5 \cdot 10^{-4}$ $mol \cdot l^{-1}$) nearly completely suppressed the action of a subsequent administration of GEA 3162 (Figure 3.4, Table 3.1).

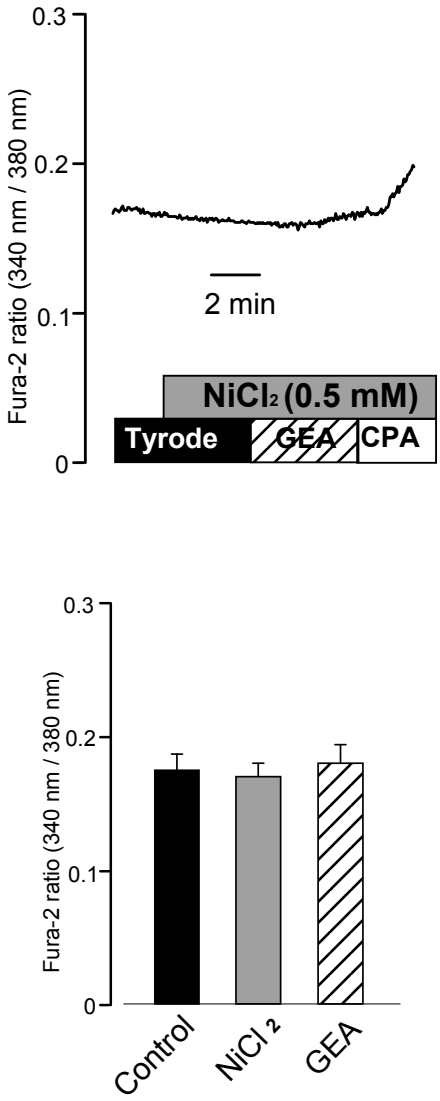

Figure 3.4: Effect of GEA 3162 (10^{-4} mol·l^{-1}) on the fura-2 ratio in the presence of the non-specific Ca^{2+}channel blocker Ni^{2+} ($5 \cdot 10^{-4}$ mol·l^{-1}) as shown in an original record (top). In average (bottom), the fura-2 ratio signal changed from 0.18 ± 0.01 under control conditions (black bar) to 0.17 ± 0.01 after the addition of Ni^{2+} (grey bar), and raised to 0.18 ± 0.01 in the presence of GEA 3162 (shaded bar; n = 16; not significant). Values are means ± S.E.M. Viability of cells was tested by the SERCA-blocker, cyclopiazonic acid ($5 \cdot 10^{-5}$ mol·l^{-1}).

A reduction of the GEA 3162 response was also observed in the presence of Co^{2+} (10^{-3} mol·l^{-1}; Figure 3.5, Table 3.1), although the effect of this divalent cation was less pronounced compared to that of Ni^{2+}.

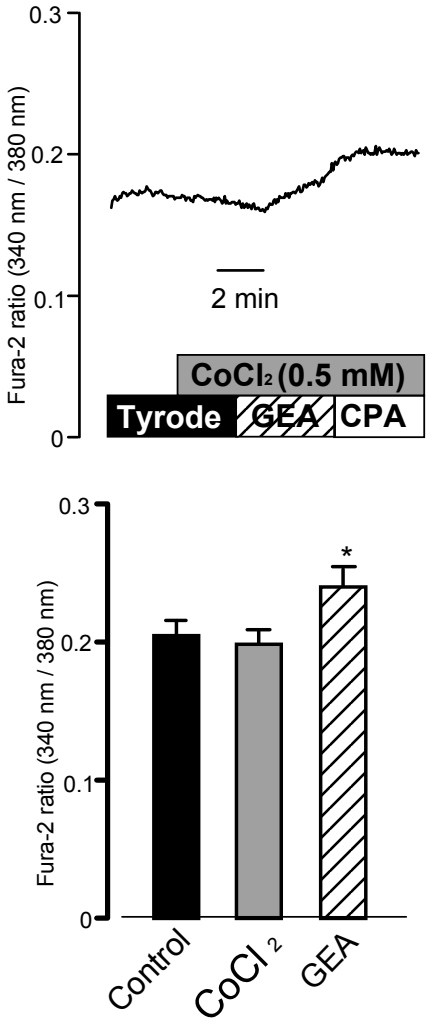

Figure 3.5: Effect of GEA 3162 (10^{-4} mol·l^{-1}) on the fura-2 ratio in the presence of the non-specific Ca^{2+} channel blocker Co^{2+} (10^{-3} mol·l^{-1}) at rat myenteric ganglia as shown in an original record (top). In average (bottom), the fura-2 ratio signal changed from 0.21 ± 0.01 under control conditions (black bar) to 0.21 ± 0.01 after the addition of Co^{2+} (grey bar), and raised to 0.25 ± 0.01 in the presence of GEA 3162 (shaded bar; n = 34). Values are means ± S.E.M., * $p < 0.05$ versus fura-2 ratio in the presence of Co^{2+}. Viability of cells was tested by SERCA-blocker, cyclopiazonic acid ($5 \cdot 10^{-5}$ mol·l^{-1}).

In order to differentiate the subtypes of the voltage-dependent Ca^{2+} channels involved, more specific inhibitors were tested. Nifedipine (10^{-6} $mol \cdot l^{-1}$) and verapamil (10^{-5} $mol \cdot l^{-1}$), two L-type channel blockers (Kochegarov 2003), exhibited a significant inhibition of the GEA 3162 action (Figures 3.6 and 3.7, Table 3.1).

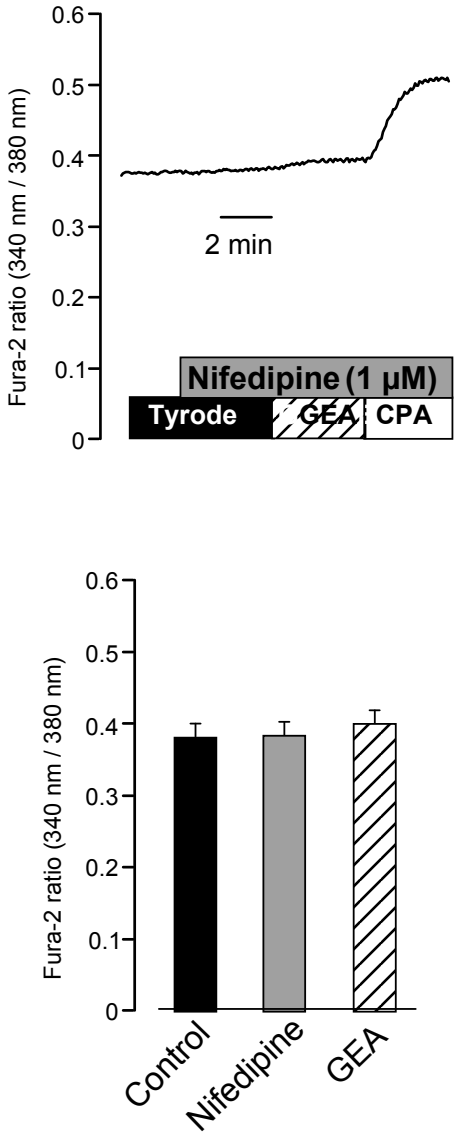

Figure 3.6: The original recording (top) demonstrates the inhibition of the GEA 3162 (10^{-4} $mol \cdot l^{-1}$)-induced increase in the fura-2 ratio by nifedipine (10^{-6} $mol \cdot l^{-1}$) at cultured myenteric ganglia of rat. The bar diagram shows the quantification of fura-2 fluorescence present in the myenteric plexus; for statistics, see Table 3.1. Results express means ± S.E.M. n = 52. Viability of cells was tested by the SERCA-blocker, cyclopiazonic acid ($5 \cdot 10^{-5}$ $mol \cdot l^{-1}$).

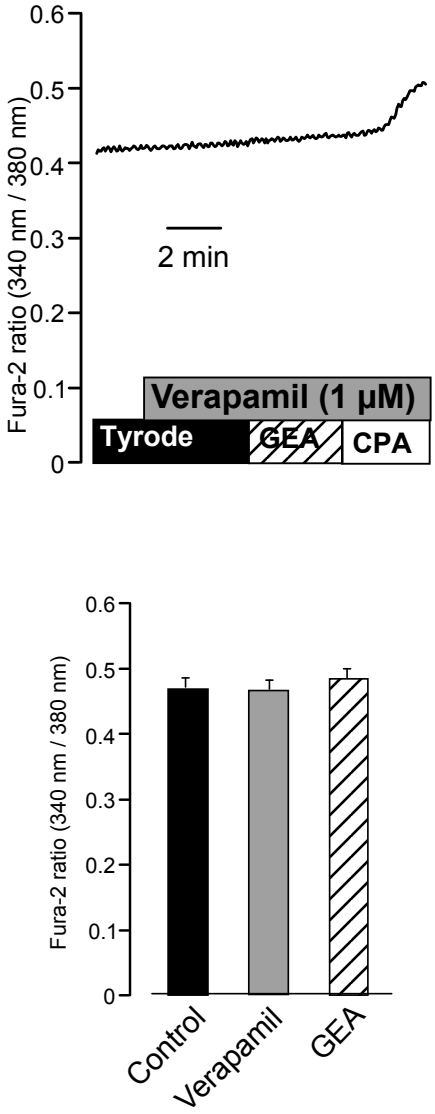

Figure 3.7: The original record (top) shows an inhibition in the GEA 3162 (10^{-4} mol·l^{-1})-induced increase of the fura-2 ratio by verapamil (10^{-5} mol·l^{-1}). The bars are showing the quantification of fura-2 fluorescence present in the myenteric plexus; for statistics, see Table 3.1. Results express means ± S.E.M., n = 38. Viability of cells was tested by the SERCA-blocker, cyclopiazonic acid ($5 \cdot 10^{-5}$ mol·l^{-1}).

In contrast, after the exposure to a N-type blocker, ω-conotoxin GVIA (10^{-6} mol·l^{-1}), only a partial reduction was observed (Figure 3.8).

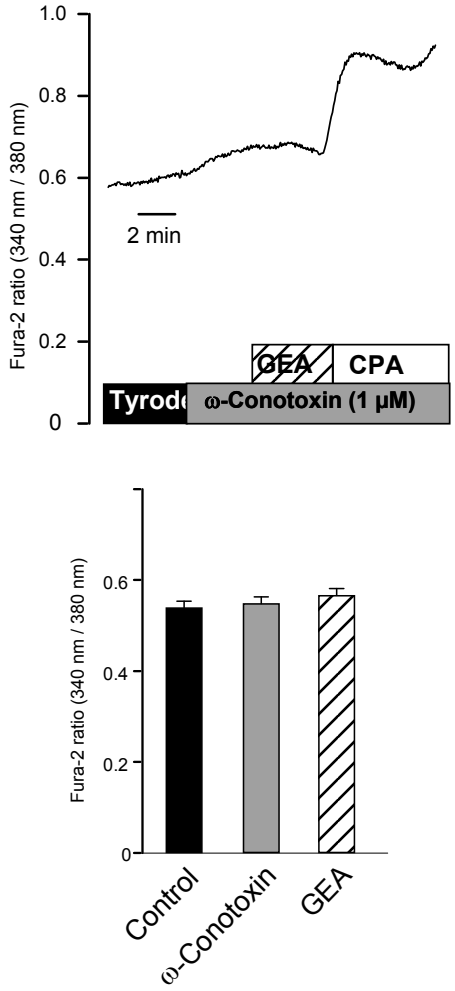

Figure 3.8: Original record representing the partially inhibition of the response to GEA 3162 (10^{-4} mol·l^{-1}) after addition of ω-conotoxin GVIA (10^{-6} mol·l^{-1}) at rat cultured myenteric ganglia (top). The grafic demonstrates the quantification of the fura-2 fluorescence present in the myenteric plexus (bottom). For statistics, see text. Results are means ± S.E.M., n = 132. Viability of cells was tested by administration of the SERCA-blocker, cyclopiazonic acid (CPA; $5 \cdot 10^{-5}$ mol·l^{-1}).

Finally, the ability of the P-type channel blocker, ω-agatoxin IVA ($2 \cdot 10^{-7}$ $mol \cdot l^{-1}$), to interfer with the GEA 3162 response was tested. However, in the presence of this 'inhibitor', a paradox potentiation of the effect of the NO donor was observed, as GEA 3162 evoked an increase in the fura-2 ratio from 0.45 ± 0.02 to 0.63 ± 0.03 (Figure 3.9, Table 3.1).

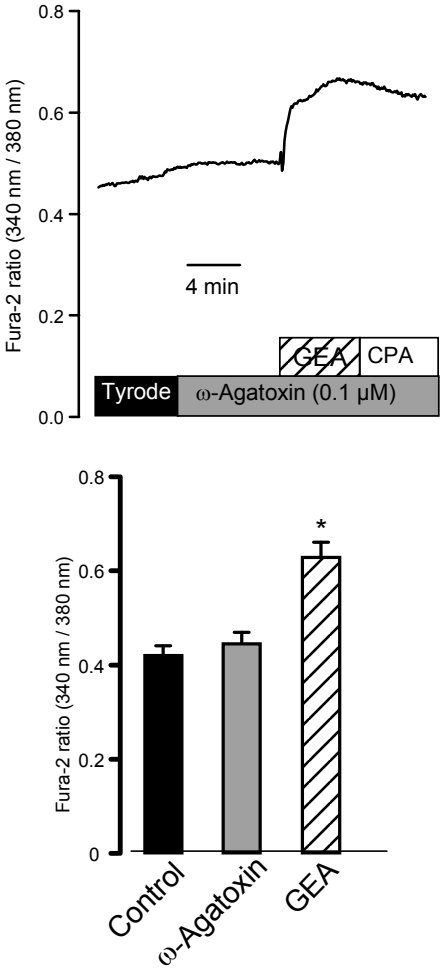

Figure 3.9: Original record representing the paradox potentiation of the GEA 3162 (10^{-4} $mol \cdot l^{-1}$)-induced increase in the fura-2 ratio after addition of ω-agatoxin IVA ($2 \cdot 10^{-7}$ $mol \cdot l^{-1}$) in rat cultured myenteric ganglia (top). The graphic gives the quantification of fura-2 fluorescence present in the myenteric plexus (bottom), for statistics, see text. Results express means ± S.E.M (n = 132), * $p < 0.05$ versus fura-2 ratio just prior administration of GEA 3162. Viability of cells was tested by administration of the SERCA-blocker, cyclopiazonic acid (CPA; $5 \cdot 10^{-5}$ $mol \cdot l^{-1}$).

Table 3.1: Effects of inhibitors on the fura-2 fluorescence ratio in rat myenteric neurones

Inhibitor	Fura-2 ratio before GEA 3162	Fura-2 ratio after GEA 3162	Δ Fura-2 ratio	n
None	0.43 ± 0.013	0.51 ± 0.018*	0.077 ± 0.013[a]	66
Ca^{2+}-free	0.23 ± 0.006	0.24 ± 0.007	0.009 ± 0.001[b]	66
Ni^{2+}	0.17 ± 0.010	0.18 ± 0.013	0.010 ± 0.004[b]	16
Co^{2+}	0.20 ± 0.010	0.24 ±0.013	0.042 ± 0.005[a,b]	34
Nifedipine	0.39 ± 0.018	0.40 ± 0.018	0.016 ± 0.001[b]	52
Verapamil	0.46 ± 0.013	0.48 ± 0.014	0.019 ± 0.002[b]	38
ω-Conotoxin GVIA	0.55 ± 0.015	0.57 ± 0.015	0.014 ± 0.003[b]	132
ω-Agatoxin IVA	0.43 ± 0.026	0.64 ± 0.035*	0.209 ± 0.023[c]	53

Fura-2 ratio before and after administration of GEA 3162 (10^{-4} mol·l^{-1}), and difference between both (Δ fura-2 ratio) in the absence of any inhibitors, in the absence of extracellular Ca^{2+}, and in the presence of Ni^{2+} (10^{-3} mol·l^{-1}), Co^{2+} ($5 \cdot 10^{-4}$ mol·l^{-1}), nifedipine (10^{-6} mol·l^{-1}), verapamil (10^{-5} mol·l^{-1}), ω-conotoxin GVIA (10^{-6} mol·l^{-1}), or ω-agatoxin IVA (10^{-7} mol·l^{-1}). Values are means ± SEM, n = number of cells tested. * $p < 0.05$ versus baseline before administration of GEA 3162. For the Δ fura-2 data, homogenous groups are indicated by identical letters (analysis of variances followed by test of Scheffé).

3.4. Identification of NOS expression in cultured myenteric ganglia by RT-PCR

If NO should exert effects on myenteric ganglia under physiological conditions, the ganglionic cells should possess the ability to produce this gaseous messenger substance. Therefore, the expression of different subtypes of the NO synthase (NOS), the enzyme responsible for the production of NO from the amino acid arginine (Moncada et al. 1989), was investigated using RT-PCR. Three different isoforms of NOS are known, i.e. nNOS, eNOS and iNOS (Xie et al. 1992, Michel and Lamas 1992, Huber et al. 1998).

Specific primers for all subtypes were used (Schricker et al. 1996). GAPDH was used as internal standard to test the quality of the PCR reaction. cDNA from rat kindey, which expresses all three isoforms of NOS (Schricker et al. 1996), was used as reference tissue.

Under basal conditions, both the mRNA for nNOS (Figure 3.10) as well as for eNOS (Figure 3.11) was found, although the latter only revealed a small, but highly reproducible band in the individual gels. Under basal conditions, iNOS expression could not be detected (data not shown).

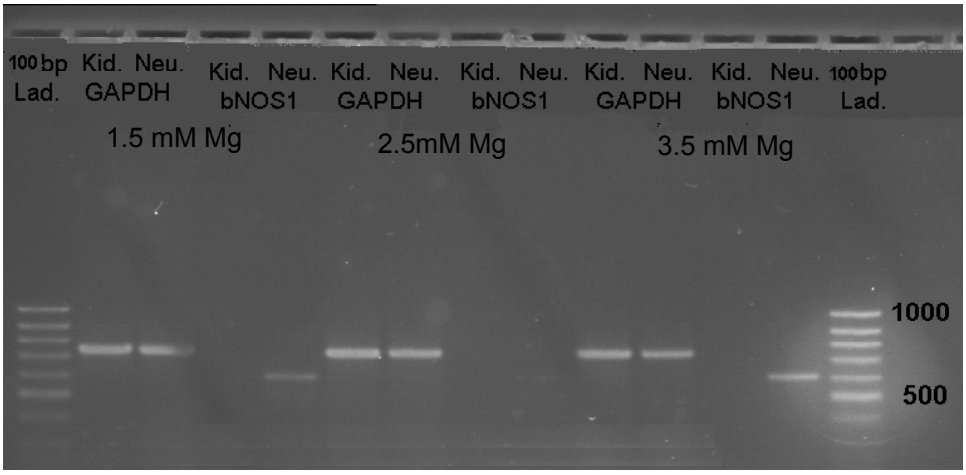

Figure 3.10: Representative gel electrophoresis image after RT-PCR for neuronal nitric oxide synthase (nNOS = bNOS) and GAPDH in cultured myenteric ganglia of rat (Neu.). Rat kidney (Kid.) served as control, Lad. = ladder ranging from 1000 to 50 bp. The nNOS primer yielded product of approximately 600 bp. Typical result from 3 independent experiments.

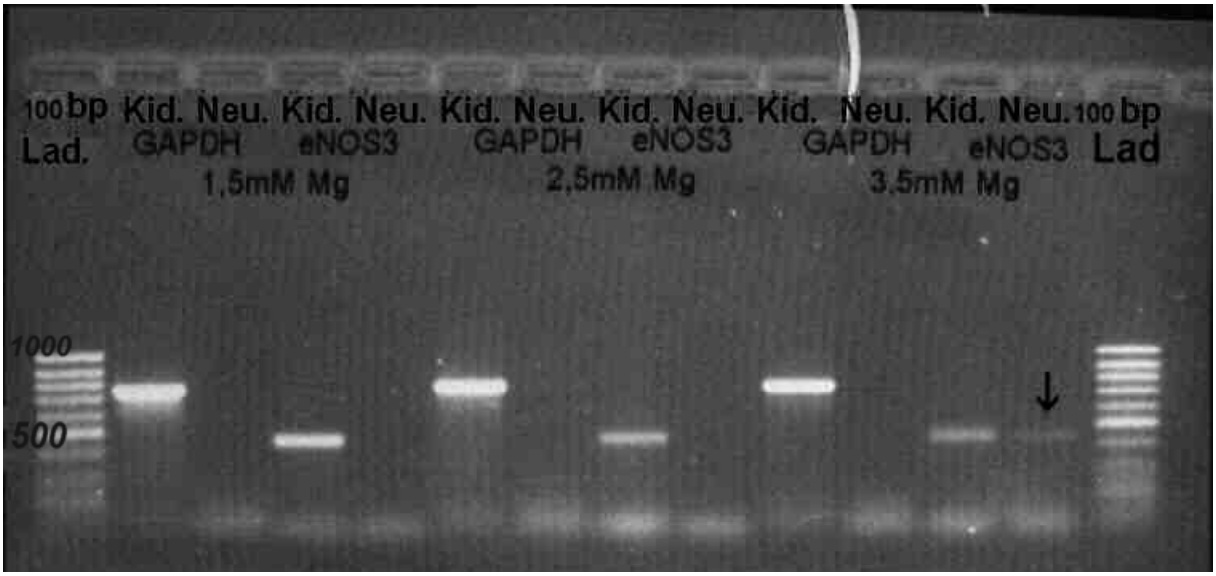

Figure 3.11: Representative gel electrophoresis image after RT-PCR for endothelial nitric oxide synthase (eNOS) and GAPDH in cultured myenteric ganglia of rat. Rat kidney (Kid.) served as control, Lad. = ladder ranging from 1000 to 50 bp. The eNOS primer yielded a product of approximately 200 bp. Typical result from 3 independent experiments.

iNOS has been proposed to be responsible for the production of NO during inflammatory reactions, because iNOS expression is induced by proinflammatory cytokines in many tissues (Wang and Marsden 1995). Therefore, in the next series of experiments, myenteric ganglia were pretreated for different time intervals with the proinflammatory cytokine, tumor necrosis factor-α (TNF-α). However, even after preexposure to TNF-α (100 ng·ml^{-1}) for 4 h, 1 d or 3 d, no mRNA for iNOS was found in the myenteric ganglia (Figure 3.12).

In the last experiment I tried using the whole tissue (longitudinal muscle layer-myenteric plexus preparation) of colon of adult rat after one day incubation with TNF-α to detect the mRNA of iNOS isoform, but cDNA obtained could not be amplified (data not shown).

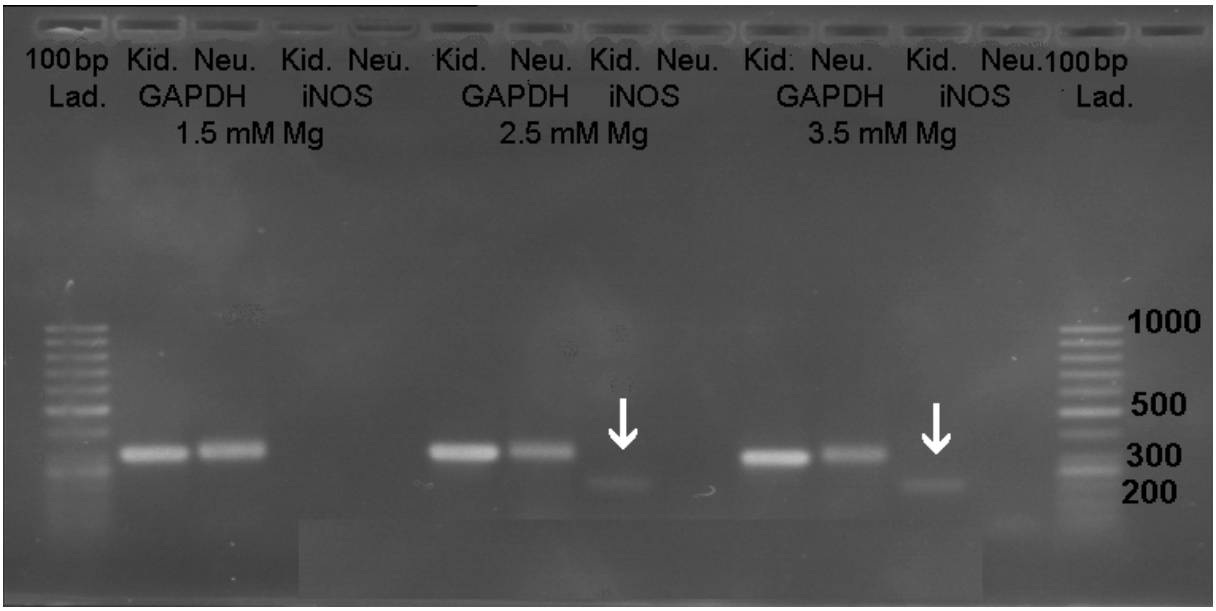

Figure 3.12: Representative gel electrophoresis image after RT-PCR for inducible nitric oxide synthase (iNOS) and GAPDH in cultured myenteric ganglia of rat (Kid.= Kidney, Neu.= Neuron). Rat kidney served as control. Arrow: basal mRNA expression of iNOS in the control probe kidney. Lad. = ladder ranging from 1000 to 50 bp. The iNOS primer yielded product of approximately 200 bp. Typical result from 3 independent experiments.

3.5. Immunohistochemistry staining

Immunohistochemical staining was used in order to localize NOS isoforms protein in the cultured myenteric ganglionic cells. Immunohistochemical studies revealed, consistent with the expression of the PCR product, the presence of both neuronal and endothelial NOS isoforms (Figure 3.13 and 3.14).

A basal expression of iNOS was not found (data not shown). However, in contrast to the PCR experiments, an immunohistochemical signal for iNOS was detected after pretreatment of the ganglia with TNF-α (Figure 3.15).

As can be seen from the overlay with the nuclear marker, DAPI, which stains the nuclei of all cells in the preparation, not all ganglionic cells were immunoreactive for the respective enzyme.

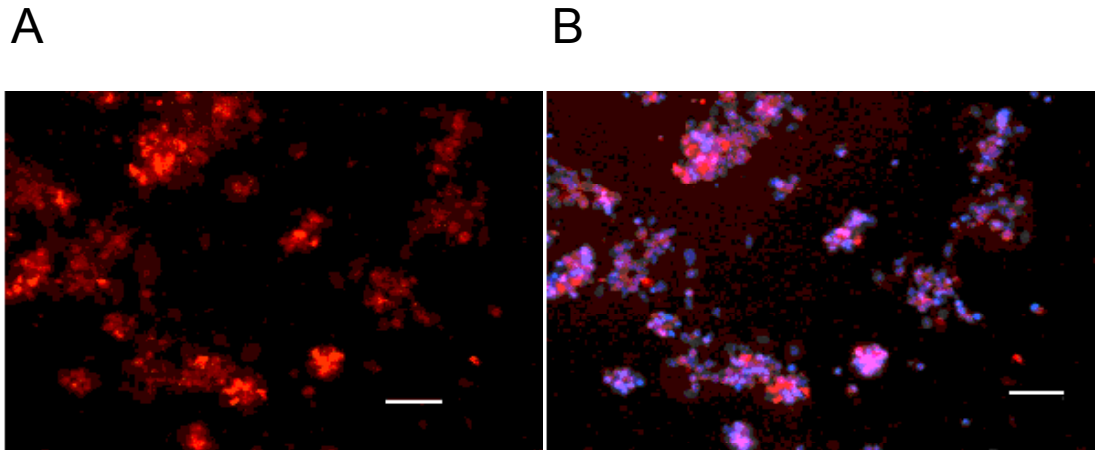

Figure 3.13: Photomicrograph of nNOS immunoreactivity in rat cultured myenteric cells. A) nNOS immunoreactivity (red); B) Overlay of the nNOS signal (red) and nuclear marker DAPI (blue). Scale bars = 50 µm.

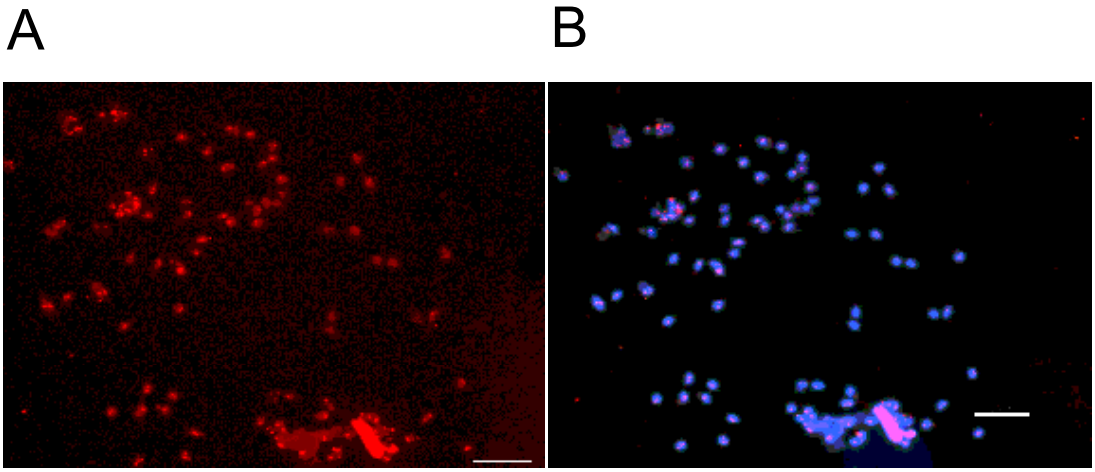

Figure 3.14: Expression of eNOS by immunohistochemistry at rat myenteric cells. A) eNOS immunoreactivity (red); B) Overlay of the eNOS signal (red) and the nuclear marker DAPI (blue). Scale bars = 50 µm.

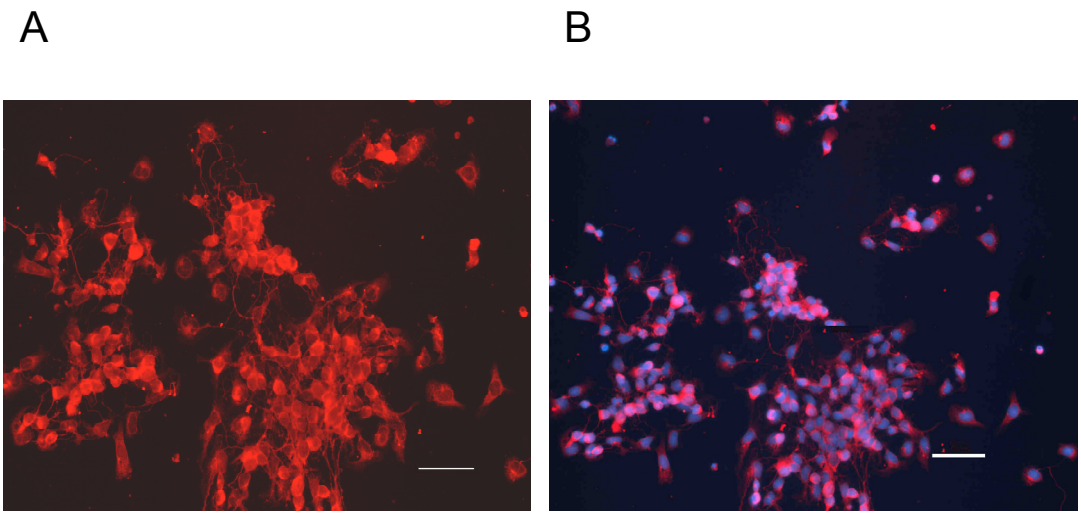

Figure 3.15: Immunoreactivity of iNOS at rat myenteric ganglia after pretreatment with TNF-α. A) iNOS immunoreactivity (red); B) overlay of the iNOS signal and the nuclear marker DAPI (blue). Scale bars = 50 µm.

In order to answer the question, whether neurons or glia cells or both express nNOS and eNOS, double labelling experiments were performed. Neurons were labelled with the neuronal marker, PGP 9.5; glial cells were marked with GFAP. These experiments were only performed for the two NOS isoforms expressed under basal conditions, i.e. nNOS and eNOS.

These experiments revealed that both PGP 9.5- as well as GFAP-positive cells expressed both isoforms of NOS (Figure 3.16 and 3.17).

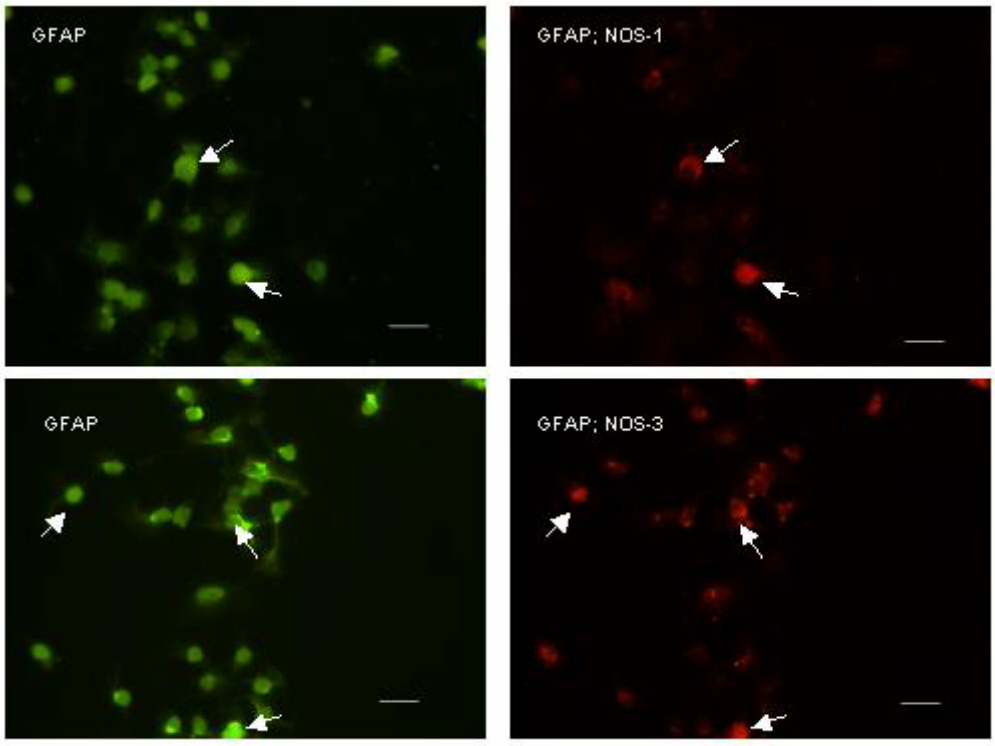

Figure 3.16: Immunoreactivity of the glial marker, glial fibrillary acidic protein (GFAP, green), and colocalization with NOS1 and NOS3 (red) immunoreactivity at rat myenteric plexus. Arrows point at double-labelled cells. Scale bars = 20μm

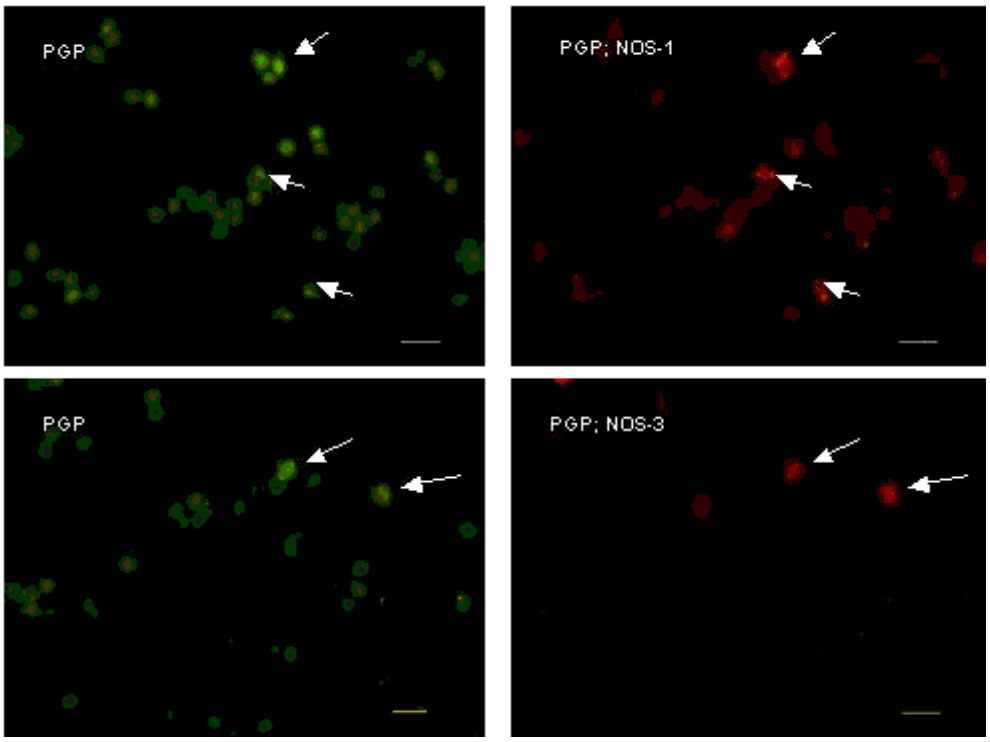

Figure 3.17: Immunoreactivity of the neuronal marker, protein gene product 9.5 (PGP 9.5; green), with NOS1 and NOS3 (red) immunoreactivity at rat myenteric plexus. Arrows point at double-labelled cells. Scale bars = 20µm

4.Discussion

4.1. Action of NO on intracellular Ca^{2+} concentration of rat myenteric ganglia

The aim of this study was to characterize the effect of the nonadrenergic-noncholinergic neurotransmitter, NO, on rat myenteric ganglia. Administration of the lipophilic NO donor, GEA 3162 (10^{-4} $mol \cdot l^{-1}$), evoked a pronounced increase in the intracellular Ca^{2+} concentration mesaured at ganglia loaded with the Ca^{2+}-sensitive fluorescent dye, fura-2 (Figure 3.1).

Despite the heterogenity of enteric neurons concerning morphology, transmitter expression, or electrophysiological properties, the response was consistently observed at the cultured myenteric ganglia, suggesting that most of these cells respond to this neurotransmitter. As already mentioned in the Introduction, myenteric neurons have been classified according to several criteria, e.g. according to shape as Dogiel type I and type II neurons, according to electrophysioloical properties as AH and S neurons, and according to function as sensory neurons, interneurons and motor neurons with different neurotransmitter expression (Wood 1994). Although the contribution of Ca^{2+} ions to the generation of action potential in AH-type neurons is pivotal, Ca^{2+} imaging studies have shown the presence of voltage-operated Ca^{2+} channels also in S-type neurons (Hanani and Ross 1997).

The increase in the cytosolic Ca^{2+} concentration caused by the NO donor was strongly reduced in the abscence of extracellular Ca^{2+} indicating the activation of Ca^{2+} influx from the extracellular space after exposure to NO (Figure 3.3). Neurons like many other cells use both extracellular and intracellular sources of calcium. The entry of Ca^{2+} from outside is regulated by voltage-operated channels or by receptor-operated channels controlled by ionotropic neurotransmitters (Berridge 1998). However, the voltage-operated channels constitute the main source of calcium in excitable cells such as neurons and muscle cells (Berridge et al. 1998).

This finding was confirmed by the inhibition of the induced Ca^{2+} signal after addition of typical blockers of voltage-gated Ca^{2+} channels such as nifedipine, suggesting that the action of NO on cytosolic Ca^{2+} of myenteric ganglia is through this type of Ca^{2+} channels.

4.2. Mechanism of action of Ca^{2+} channel blockers

Calcium channel blockers (or antagonists), which I used as tools, refer to a chemically, pharmacologically and therapeutically heterogeneous group of drugs used either e.g. as cardiovascular therapeutic agents or as molecular tools (Triggle 2007). Nifedipine is the prototype of the dihydropyridine group. It contains in its molecular structure one dihydropyridine and one benzene cycle (Figure 4.1). Verapamil, belonging to the phenylalkylamines, consists of two benzene cycles

connected by a carbohydrate chain with one nitrogen atom (Figure 4.2). The mechanism, by which calcium channel blockers function, has been proposed to be via binding in the pore of the channels and initiating conformational changes rendering the channel non-conducting. Thereby they slow down recovery of calcium channels fom voltage-induced inactivation (Kochegarvo 2003). Sanguinetti and Kass (1984) suggested that verapamil reaches the Ca^{2+} channels from the cytoplasm, whereas nifedipine acts at an extracellular side and preferentially binds to the channel in the inactivated state. Verapamil and nifedipine are traditionally used for treatment of cardiovascular diseases, e.g. as vasodilators in hypertension acting through relaxation of smooth muscle of blood vessels and reduction in blood pressure. They are also used in other disorders such as angina pectoris and arrythmia (Epstein 2002).

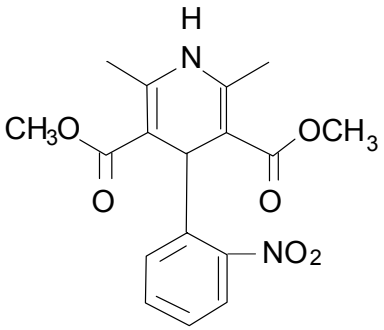

Figure 4.1: Structure of nifedipine. From Wikipedia.org

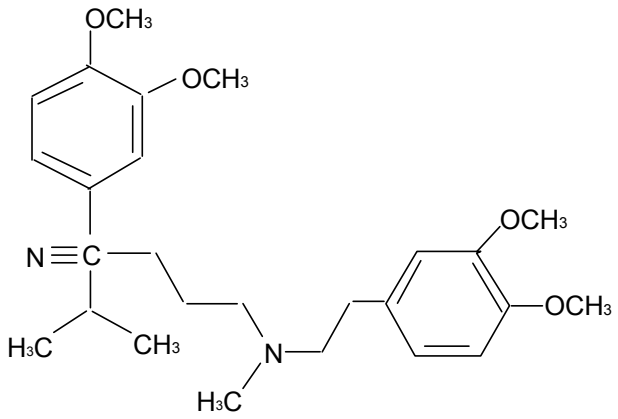

Figure 4.2: Structure of verapamil. From Wikipedia.org

The toxin peptides ω-conotoxin GVIA and ω-agatoxin IVA have been isolated from the venom of the snail Conus geographus and the funnel web spider Agelenopsis aperta, respectively. These animals use these toxins to paralyze their victims (Jones et al. 2001, McDonough et al. 2002). Conotoxins act by inhibiting presynaptic N-type calcium channels thereby preventing neurotransmitter release. They are useful tools for the block and for the study of synaptic transmission. In contrast, SNX-111 is a synthetic analog of ω-conotoxin MVIIA. It was developed for treatment of acute pain. These toxin peptides are structurally composed of amino acid residues that have short sites as short as dipeptide responsible for binding and blockade of calcium channels (Kochegarvo 2003; Figure 4.3). ω-agatoxin IVA has been found to be a potent blocker of P-type calcium channels in cerebellar Purkinje neurons which are

insensitive to both dihydropyridines and ω-conotoxin GVIA and since has been termed P-type calcium current blocker (Noony et al. 1997).

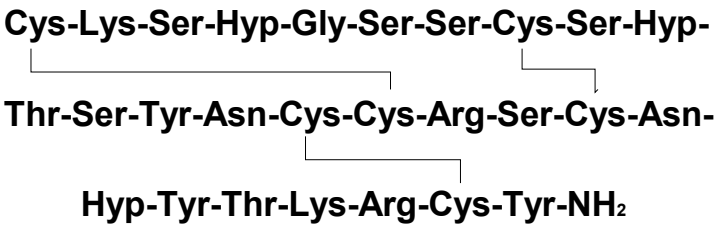

Figure 4.3: The peptide calcium channel blocker ω-conotoxin GVIA. From www.tocris.com/dispprod.php

The mechanism of Ca^{2+} channel blockade by the divalent cations Ni^{2+} and Co^{2+} has been shown to be throughout the competition with the permeating ion, Ca^{2+}. This process seems to take place within the channel itself, because these cations have a high affinity to divalent cation binding site, i.e. they stick in the pore of the channel and block permeation by other ions (Pelzer et al. 1990). The divalent cations Ni^{2+} and Co^{2+} are non-specific blockers of calcium channels, however, a high sensitivity of R-currents, which are resistant to other known Ca^{2+} channel blockers, has been shown (Noony et al. 1997, Bian et al. 2004).

My results concerning the action of NO on cytosolic Ca^{2+} in myenteric ganglia conflict with data from previous studies at other tissues, as in

bovine chromaffin cells (Carabelli et al. 2002), in rat cardiac cells (Hu et al. 1997), in rat dorsal root ganglion neurons (Yoshimura et al. 2001) and in rat cortical neurons (Petzold et al. 2005) it was reported that NO inhibits the activities of voltage-gated Ca^{2+} channels. However, in agreement with my findings, studies in rat sympathetic neurons (Chen and Schofield 1995) or in retinal ganglion cells (Hirooka et al. 2000) revealed that NO activates these channels. The discrepancy between these studies is difficult to explain and could attribute to the different types and concentrations of NO donors used, the cell types studied and different experimental procedures (Petzold et al. 2005). Another explanation might contribute to the controversial effect of NO on voltage-gated Ca^{2+} channels: NO may affect the channel activity by different mechanisms, since a direct effect by S-nitrosylation and an indirect effect by guanylate cyclase pathway have been suggested (Campbell et al. 1996). This hypothesis is supported by the observation that NO directly activates P/Q type Ca^{2+} channels (Chen et al. 2002), whereas the NO-induced production of cGMP inhibits these channels (Grassi et al. 1999).

The data obtained in the present study demonstrate that L-type Ca^{2+} channels are the major pathway for the NO effect on Ca^{2+} entry in rat myenteric ganglia, because the two L-type Ca^{2+} channels blockers tested, nifedipine and verapamil, had a strong inhibitory action on the stimulation of the Ca^{2+} influx induced by the NO donor. This finding is

supported by earlier pharmacological studies at rat myenteric ganglia showing that L- and N-type Ca^{2+} channels seem to be the most important Ca^{2+} influx pathways at these cells (Schäufele and Diener 2005). However, Bian et al. (2004) obtained evidence that R-type Ca^{2+} channels make the largest contribution to the total Ca^{2+} current in myenteric neurons of guinea pig small intestine which may reflect species-differences in neuronal Ca^{2+} channel expression.

The paradox effect of ω-agatoxin on P-type Ca^{2+} current (Figure 3.9) on rat myenteric ganglia is difficult to explain. The P-type Ca^{2+} current is well known from other nervous tissues to be sensitive to ω-agatoxin. For example, Zaitsev et al. (2007) and Santiago et al. (2008) reported that this blocker significantly inhibited the Ca^{2+} current mediated by P-type Ca^{2+} channels in rat brain neurons. An explanation for this conflicting result has been described to be due to the insensitivity of P-type current in some enzymatically dissociated neurons to typical Ca^{2+} blockers (Regan 1991, Mintz et al. 1992, Tringham et al. 2008). However, in previous experiments in our laboratory at rat myenteric ganglia using the same approach as used in this study, an inhibitory effect of the ω-agatoxin blocker on P-type Ca^{2+} current has been shown (Schäufele and Diener 2005).

Further studies are needed to investigate the mechanism by which NO affects Ca^{2+} signalling in myenteric ganglia and to clarify whether Ca^{2+} influx through voltage-gated Ca^{2+} channels induced by NO is amplified

by Ca^{2+} release from the intracellular stores through the mechanism Ca^{2+}-induced Ca^{2+} release via ryanodine and IP_3 receptors. The inositol trisphosphate receptors (IP_3Rs) and ryanodine receptors (RYRs) at the endoplasmic reticulum contribute to the Ca^{2+} signalling, as both are sensitive to Ca^{2+} entering from the extracellular space through either voltage-operated or receptor-operated Ca^{2+} channels. This calcium provides the "trigger Ca^{2+}" to stimulate Ca^{2+} release from the internal stores of the endoplasmic reticulum. This so-called Ca^{2+}-induced Ca^{2+} release is often responsibe for amplifying Ca^{2+} signals coming from the outside (Miller 1991, Barish 1991).

There is an interesting possibility of a positive feed-back loop between cytosolic Ca^{2+} and NO: Two isoforms of NO synthases (nNOS and eNOS) are Ca^{2+}-dependent. Consequently, the increase in the cytosolic Ca^{2+} concentration induced by NO might induce a further stimulation of NO production as already suggested for some other cells (Publicover et al. 1993, Moncada et al. 1991).

4.3. Functional role of NO in the myenteric plexus

An inhibitory role of nitric oxide on enteric neurons has been identified. Yuan and his coworkers (1995) found that NO plays a role in retrograde transmission between interneurons and sensory neurons as NO released from descending interneurons, which are involved in the descending pathway of the peristaltic reflex, acts back on the sensory

neurons to inhibit neurotransmission. Therefore, they concluded that NO can modulate intestinal motor reflexes via an action on neurons. Moreover, it has been reported that NO suppresses noncholinergic slow excitatory postsynaptic potentials by suppression of the release of neurotransmitters presynaptically at the slow excitatory synapses in myenteric neurons of guinea pig small intestine (Tamura et al. 1993). In addition, the presence of NOS immunoreactivity both in the cell bodies and in the nerve terminals that make synaptic contacts with other myenteric neurons indicated a possible role of NO as an ortho- or a retrograde neurotransmitter within the myenteric plexus (Bredt et al. 1990).

Given the inhibitory action of nitric oxide on myenteric neurons, a finding has come from our laboratory using the patch clamp technique to examine NO action on cell membrane potential of myenteric neurons indicating that NO hyperpolarizes the cell membrane. This hyperpolarization is related to activation of Ca^{2+}-dependent K^{+} channels (Sitmo et al. 2007). The effect of NO on membrane potential was inhibited after blockade of K^{+} channels by Cs^{+}. Thus, this observation might explain the inhibitory effect of NO on cell excitability of myenteric neurons.

We can conclude from the forementioned data that the nonadrenergic noncholinergic neurotransmitter nitric oxide affects myenteric ganglia by stimulation of voltage-dependent Ca^{2+} channels, predominantly of the

L-type. This causes the opening of Ca^{2+}-dependent K^+ channels and a hyperpolarization of the cell membrane.

If myenteric ganglia are exposed to NO released from nonneural sources, as from immune inflammatory cells in the gastrointestinal tract during inflammatory conditions, and if the principle action is expected to be suppression of cell excitability postsynaptically or an inhibition of slow synaptic excitation at presynaptic site, the question arises, what is the pathophysiological relevance of this action of NO?

NO has been identified to be one of the neuromodulators released in a paracrine fashion in inflammatory states by immune cells such as mast cells. Electrophysiological studies on enteric neurons confirm that these inflammatory mediators alter the electrical and synaptic behavior of enteric neurons. For example, the release of histamine and serotonin from mast cells in response to invading organisms affects the neural elements of the enteric nervous system, which respond by running a defense program designed to eliminate the antigens from the lumen. Copious secretion and increased blood flow followed by orthograde power motor propulsion of the luminal contents are the output of the neural program (Wood 2004). Nitric oxide has been defined to have an inhibitory action on enteric neurons and intestinal musculature. The role of NO in inflammatory states is still unknown. However, it has been shown that NO inhibits norepinephrine release from myenteric neurons thereby removing the sympathetic inhibition of secretomotor neurons,

which might contribute to secretory diarrhoea during inflammation (Rühl and Collins 1997). In general, the inflammatory process in the bowl is complex and does not function through a single pathway and the mechanism of inflammation and repair may require many, all, or none of the NO responses (Valentine et al. 1996).

4.4. Nitric oxide synthases in the myenteric plexus

The second object of the present study was to determine the expression of NOS isoforms, i.e. the forms of the enzyme responsible for NO production under physiological and pathophysiological conditions. Assessment of nNOS and eNOS by RT-PCR and immunohistochemistry revealed the presence of both enzymes in myenteric ganglia under basal conditions (Figures. 3.10, 3.11, 3.13, 3.14), whereas the inducible NOS (iNOS) could only be shown by immunohistochemistry assay and only after pretreatment with the proinflammatory cytokine, TNF-α (Figures. 3.12; 3.15). Tumor necrosis factor-α (TNF-α) is a proinflammatory cytokine produced by many cell types including macrophages, monocytes or lymphocytes in response to infection, inflammation and other environmental challenges. The molecular mechanism by which TNF-α mediates cellular responses is thought to be through binding to its two receptors, TNFR1 and TNFR2. This binding leads to activation of distinct effectors which, in turn, leads to activation of nuclear transcription factors such as AP-1 and NF-κB,

that induce genes involved in inflammatory responses (Baud and Karin 2001).

NF-κB has been shown to be related to the activation of the inducible form of nitric oxide synthase (iNOS). NF-κB under basal conditions is sequestered in the cytoplasm as an inactive complex bound to its inhibitor protein IκB. A variety of different stimuli, including bacterial products, inflammatory cytokines, and oxidants activate this transcription factor. Once activated, NF-κB translocates to the nucleus of the cell where it binds to different agents and activates the transcription of genes known to be important in the immune and inflammatory response including the regulation of the transcription of the enzyme iNOS. Thus, the production of NO increases in inflammatory states (Pavlick et al. 2002).

In contrast to the immunohistochemical experiments, I was not able to identify the mRNA for iNOS, even after pretreatment with TNF-α (Figure 3.12). The most plausible explanation for this failure is the different life time of mRNA and cellular proteins. In other words, the “time windows” after administration of TNF-α, in which I looked for this mRNA, was not adequate to register the expected transient upregulation of iNOS mRNA, which should preceed the increase in the expression of the iNOS protein.

The inducible NOS is believed to represent the major source of NO in inflammatory bowel disease (Kimura et al. 1998). It was found to be

expressed in response to inflammatory cytokines such as IL-1β and bacterial products (e.g. lipopolysaccharides) by immune cells such as macrophages and neutrophils and by myenteric neurons (Xie et al. 1992, Valentine et al. 1996). Overproduction of NO during intestinal inflammation has been identified (Lundberg et al. 1994, Cross and Wilson 2003). However, studies examining the role of NO in inflammatory states of the gut have revealed conflicting results and the mechanism by which iNOS exerts its effects remains unclear (Vallance et al. 2004). iNOS production by macrophages and other phagocytes is thought to primarily act as an antimicrobial mechanism that helps to destroy bacteria. However, the excess of reactive oxygene species (ROS) produced by activated immune cells and myenteric cells after exposure to cytokines under inflammatory conditions and the induction of NO production via iNOS may provide a neuroprotective role by scavenging the excess oxygen radicals by a mechanism thought to be mediated through the reaction with superoxide anions (O_2^-) to generate peroxynitrite (Beckmann et al. 1990), which may contribute to intestinal damage in gut inflammation.

iNOS immunoreactivity was observed also in most ganglionic cells (Figure 3.15) sugessting that also the glial cells, which constitute about half of the ganglionic cells, respond to the proinflammatory cytokine TNF-α by producing NO. An evidence supports this finding in a dextran sodium sulfate-induced colitis model, where iNOS glial immunoreactivity

has been found. The authors imply a role for these cells in the modulation of epithelial Cl^- transport (Green et al. 2004).

The presence of nNOS and eNOS in the myenteric plexus has been demonstrated by other studies (Bredt et al. 1990, Aimi et al. 1993). However, immunohistochemical studies in guinea-pig gastrointestinal tract have shown that NOS is found in inhibitory motor neurons innervating circular muscle and in descending interneurons, but not in cells that have been identified electrophysiologically as sensory neurons (Yuan et al. 1995). These enzymes are activated only during periods of activation in normal physiological responses when cytoplasmic Ca^{2+} concentration rises and the NO released by them acts as a transduction mechanism underlying physiological response (Sanders and Ward 1992). For example, NO released by eNOS in endothelial cells in response to stimulation by acetylcholine acts to relax blood vessels and to increase the blood flow to the tissues. Nitric oxide released by nNOS in response to nerve stimulation of the myenteric plexus causes relaxation of the gastrointestinal smooth muscles, which plays an important physiological role in various parts of the gastrointestinal tract. Nitric oxide regulates e.g. the muscle tone of the sphincter in the lower esophagus, the pylorus and the anus and regulates the accomodation reflex of the stomach and the peristaltic reflex of the intestine (Takahashi 2003). However, recent reports have shown eNOS and nNOS to be also of pathophysiological significance. Synthesis of NO in

myenteric neurons by nNOS during early experimental endotoxemia has been suggested to be involved in stomach hypocontractility and hypothesized to maxime the neural activity bevor the recruitment of immune response through iNOS (Quintana et al. 2004). Vallance and coworkers (2004) reported in experimental colitis that the eNOS isoform plays a role for mucosal integrity, because eNOS knockout mice developed severe colitis with fewer goblet cells compared with wild-type animals.

Glial cells showed bNOS as well as eNOS immunoreactivity under basal conditions (Figure 3.16), demonstrating that these cells may well affect neighbouring neurons via NO.

In summary, my results demonstrate that NO, which can be physiologically produced within myenteric neurons, affects excitability of the myenteric neurons via a stimulation of voltage-dependent Ca^{2+} channels.

5. Summary

In this work I investigated the myenteric plexus of the rat small intestine with regard to the effects of the nonadrenergic-noncholinergic neurotransmitter, nitric oxide (NO). The action of NO on the intracellular calcium concentration $[Ca^{2+}]_i$ of myenteric ganglionic cells was measured with imaging experiments; the presence of the enzyme responsible for synthesis of NO, i.e. the nitric oxide synthases, was investigated with polymerase chain reaction and immunohistochemical experiments.

Myenteric ganglia from 5 - 12 days old rats were enzymatically isolated and kept for about 15 h under cell culture conditions. Changes in $[Ca^{2+}]_i$ were measured by loading the ganglia with the Ca^{2+}-indicator fluorescence dye, fura-2, and exposure to the NO donor, GEA 3162 (10^{-4} mol·l^{-1}). The NO donor induced a pronounced increase in $[Ca^{2+}]_i$. This increase was reduced in the absence of extracellular Ca^{2+} and after exposure to blockers of voltage-operated Ca^{2+} channels, indicating that the effect of NO on $[Ca^{2+}]_i$ is via activation of this type of Ca^{2+} channels. L- and N-type Ca^{2+} channels seem to play the dominant role by which NO induces changes in $[Ca^{2+}]_i$, since the blockers nifedipine and ω-conotoxin caused the most effective inhibition in fura-ratio signal evoked by NO.

PCR and immunohistochemical experiments revealed the presence of both neuronal and endothelial nitric oxide synthase isoforms in myenteric cells. The inducible isoform was shown by immunohistochemical experiments after

incubation of the cells with the proinflammatory cytokine, TNF-α, indicating that NO is physiologically produced within myenteric ganglia.

6. Zusammenfassung

Im Rahmen dieser Arbeit wurde die Wirkung des nonadrenergen-noncholinergen Neurotransmitters Stickstoffmonooxid (NO) auf Zellen des Plexus myentericus der Ratte untersucht inklusive der Expression der Enzyme, die für die Produktion dieses Neurotransmitter verantwortlich sind.

Myenterische Ganglien von 5 bis 12 Tage alten Ratten wurden enzymatisch isoliert und nach ca. 15 Stunden in Kultur mit dem Ca^{2+}-Indikator Fura-2-AM beladen. Die intrazelluläre Ca^{2+}-Konzentration ($[Ca^{2+}]_i$) wurde mit der Imaging Methode gemessen.

Imaging Experimente zeigten, dass der NO Donor GEA 3162 (10^{-4} $mol \cdot l^{-1}$) einen signifikanten Anstieg der intrazellulären Calciumkonzentration verursachte. Dieser Anstieg ist durch Aktivierung spannungsabhängiger Ca^{2+}-Kanäle verursacht, da der NO-Effekt in Abwesenheit von extrazellulärem Ca^{2+} oder nach Zugabe von Blockern von spannungsabhängigen Ca^{2+}-Kanälen stark gehemmt war.

Der Einfluss von GEA 3162 auf myenterische Zellen der Ratte scheint durch L- und N-Typ spannungsabhängige Ca^{2+}-Kanäle vermittelt zu sein, denn die Hemmstoffe dieser Ca^{2+}-Kanäle, Nifedipin bzw. ω-Conotoxin, erwiesen sich als die wirksamsten, um den NO-bedingten Anstieg von ($[Ca^{2+}]_i$) zu vermindern.

Polymerasekettenreaktions- (PCR-) und immunhistochemische Versuche wiesen die Existenz mehrerer Isoformen des Enzyms NO

Synthase, nämlich der neuronalen Form (nNOS) und der endothelialen Form (eNOS), nach. Die dritte Isoform, die induzierbare NOS (iNOS), konnte nur mit immunhistochemischen Versuchen nach Stimulation der Ganglien mit dem proinflammatorischen Zytokin TNF-α nachgewiesen werden. Diese Versuche zeigen, dass NO unter physiologischen Bedingungen im Plexus myentericus gebildet werden kann.

7. References

Aimi Y, Kimura H, Kinoshita T, Minami Y, Fujimura M, Vincent SR. Histochemical localization of nitric oxide synthase in rat enteric nervous system. Neuroscience 53: 553-56, 1993

Altdorfer K, Bagam'eri G, Donath T, Feher E. Nitric oxide synthase immunoreactivity of interstitial cells of Cajal in experimental colitis. Inflamm Res 51: 569-571, 2002

Arnold WP, Mittal CK, Katsuki S, Murad F. Nitric oxide activates guanylate cyclase and increases guanosine 3':5'-cyclic monophosphate levels in various tissue preparations. Proc Natl Acad Sci USA 74: 3203-3207, 1977

Barish ME. Increases in intracellular calcium ion concentration during depolarization of cultured embryonic Xenopus spinal neurons. J Physiol 444: 545-565, 1991

Baud V, Karin M. Signal transduction by tumor necrosis factor and its relatives. Trends Cell Biol 11: 372-377, 2001

Bayliss WM, Starling EH. The movements and innervation of the small intestine. J Physiol 24: 100-143, 1899

Baylor SM, Hollingworth S. Measurement and interpretation of cytoplasmic [Ca^{2+}] signals from calcium-indicator dyes. News Physiol Sci 15: 19-26, 2000

Bean BP. Classes of calcium channels in vertebrate cells. Annu Rev Physiol 51: 367-384, 1989

Beckman JS, Beckman TW, Chen J, Marshall PA, Freeman BA. Apparent hydroxyl radical production by peroxynitrite: implications for endothelial injury from nitric oxide and superoxide. Proc Natl Acad Sci USA 87: 1620-1624, 1990

Beckman JS, Koppenol WH. Nitric oxide, superoxide, and peroxynitrite: the good, the bad, and ugly. Am J Physiol Cell Physiol 271: C1424-C1437, 1996

Berghe PV, Missiaen L, Janssens J, Tack J. Calcium signalling and removal mechanisms in myenteric neurones. Neurogastroenterol Mot 14: 63-73, 2002

Berridge MJ, Bootman MD, Lipp P. Calcium a life and death signal. Nature 395: 645-648, 1998

Berridge MJ. Neuronal calcium signaling. Neuron 21: 13-26, 1998

Berthoud HR, Jedrzejewska A, Powley TL. Simultaneous labeling of vagal innervation of the gut and afferent projections from the visceral forebrain with Dil injected into the dorsal vagal complex in the rat. J Comp Neurol 301: 65-79, 1990

Berthoud HR, Kressel M, Raybould HE, Neuhuber WL. Vagal sensors in the rat duodenal mucosa: distribution and structure as revealed by in vivo Dil-tracing. Anat Embryol 191: 203-212, 1995

Berthoud HR, Neuhuber WL. Functional and chemical anatomy of the afferent vagal system. Auton Neurosci Basic Clin 85: 1-17, 2000

Berthoud HR, Powley TL. Vagal afferent innervation of the rat fundic stomach: morphological characterization of the gastric tension receptor. J Comp Neurol 319: 261-276, 1992

Bian X, Zhou X, Galligan JJ. R-type calcium channels in myenteric neurons of guinea pig small intestine. Am J Physiol Gastrointest Liver Physiol 287: G134-G142, 2004

Bodian M, Stephens FD, Ward BCH. Hirschsprung's disease and idiopathic megacolon. Lancet 1: 6-11, 1949

Bornstein JC, Costa M, Furness JB, Lees GM. Electrophysiology and Enkaphalin immunoreactivity of identified myenteric plexus neurons of guinea-pig small intestine. J Physiol 351: 313-325, 1984

Bredt DS, Hwang PM, Snyder SH. Localization of nitric oxide synthase indicating a neural role for nitric oxide. Nature 347: 768-770, 1990

Busse R, Mulsch. Calcium-dependent nitric oxide synthesis in endothelial cytosol is mediated by calmodulin. FEBS Lett 265: 133-136, 1990

Calignano A, Whittle JR, Di Rosa M, Moncada S. Involvement of endogenous nitric oxide in the regulation of rat intestinal motility in vivo. Eur J Pharmacol 229: 273-276, 1992

Campbell DL, Stamler JS, Strauss HC. Redox modulation of L-type calcium channels in ferret ventricular myocytes: Dual mechanism regulation by nitric oxide and S-nitrosothiols. J Gen Physiol 108: 277-293, 1996

Carabelli V, Ascenzo MD, Carbone E, Grassi C. Nitric oxide inhibits neuroendocrine Ca1 L-channel gating via cGMP-dependent protein kinase in cell-attached patches of bovine chromaffin cells. J Physiol 541: 351–366, 2002

Cattell V, Jansen A. Inducible nitric oxide synthase in inflammation. Histochem J 27: 777-784, 1995

Catterall WA, Striessnig J, Snutch TP, Perez-Reyes E. International union of pharmacology. XL. Compendium of voltage-gated ion channels: Calcium channels. Pharmacol Rev 55: 579-581, 2003

Catterall WA. Structure and regulation of voltage-gated Ca^{2+} channels. Annu Rev Cell Dev Biol 16: 521-555, 2000

Chen C, Schofield GG. Nitric oxide donors enhanced Ca^{2+} currents and blocked noradrenaline-induced Ca^{2+} current inhibition in rat sympathetic neurons. J Physiol 482: 521–531, 1995

Chen J, Daggett H, Waard Mde, Heinemann SH, Hoshi T. Nitric oxide augments voltage-gated P/Q-type Ca^{2+} channels constituting a putative positive feedback loop. Free Radical Biol Med 32: 638–649, 2002

Clementi E. Role of nitric oxide and its intracellular signalling pathways in the control of Ca^{2+} homeostasis. Biochem Pharmacol 55: 713-718, 1998

Costa M, Brookes SJH, Hennig GW. Anatomy and physiology of the enteric nervous system. Gut 47: 15-19, 2000

Costa M, Furness JB, Llewellyn-Smith IJ, Cuello AC. Projections of substance P neurons within the guinea-pig small intestine. Neuroscience 6: 411-424, 1986

Costa M, Waterman S, Brookes SJH. The role of nitric oxide synthesizing enteric neurons in peristalsis in the guinea-pig small and large intestine (Abst.). Proc Aust Physiol Pharmacol Soc 22: 98, 1991

Cross RK, Wilson KT. Nitric oxide in inflammatory bowel disease. Inflamm Bowel Dis 9: 179-189, 2003

Daniel EE, Jury J, Salapatek AM, Bowes T, Lom A, Thomas S, **Ramnarain M, Nguyen V, Mistrv V**. Nitric oxide from enteric nerves acts by a different mechanism from myogenic nitric oxide in canine lower esophageal sphincter. J Pharmacol Exp Ther 294: 270-279, 2000

Dawson TM, Bredt DS, Fotuhi M, Hwang PM, Snyder SH. Nitric oxide synthase and neuronal NADPH diaphorase are identical in brain and peripheral tissues. Proc Natl Acad Sci USA 88: 7797-7801, 1991

Derkach V, Surprenant A, North RA. 5-HT3 receptors are membrane ion channels. Nature 339: 706-709, 1989

Dogiel AS. Über den Bau der Ganglien in den Geflechten des Darmes und der Gallenblase des Menschen und der Säugetiere. Arch Anat Physiol Leipzig Anat Abt 130-158, 1899

Drew GM. Pharmacological characterization of the presynaptic α-adrenoceptors regulating cholinergic activity in the guinea-pig ileum. Br J Pharmacol 64: 293-300, 1978

Epstein M. In: Epstein M, editor. Calcium antagonists in clinical medicine. 3rd ed., philadelphia, PA: Hanley and Belfus, 2002

Fox EA, Phillips RJ, Martinson FA, Baronowsky EA, and Powley TL. Vagal afferent innervation of smooth muscle in the stomach and duodenum of the mouse: morphology and topography. J Comp Neurol 428: 558-576, 2000

Furness JB, Costa M. The enteric nervous system. London/NewYork: Churchill Livingston, 1987

Galione A. Cyclic ADP-ribose, the ADP-ribosyl cyclase pathway and calcium signaling. Mol Cell Endocrinol 98: 125-131, 1994

Garg UC, Hassid A. Nitric oxide decreases cytosol free calcium an balb/c3T3 fibroblasts by a cyclic GMP-independt mechanism. J Biol Chem 266: 9-12, 1991

Garthwait J, Charles SL, Chess-Williams R. Endothelium derived relaxing factor release on activation of NMDA receptors suggests role as intercellular messenger in the brain. Nature 336: 385-388, 1988

Gershon MD. The enteric nervous system. Ann Rev Neurosci 14: 227-272, 1981

Gonella J, Bouvier M, Blanquet F. Extrinsic nervous control of motility of small and large intestines and related sphincters. Physiol Rev 67: 902-961, 1987

Grafe P, Mayer CJ, Wood JD. Evidence that substance P does not mediate slow synaptic excitation within the myenteric plexus. Nature 279: 720-721, 1979

Grassi CD, Ascenzo M, Valente A, Battista Azzena G. Ca^{2+} channel inhibition induced by nitric oxide in rat insulinoma RINm5f cells. Pflugers Arch 437: 241-247, 1999

Green CL, Ho W, Sharkey KA, McKay DM. Dextran sodium sulfate-induced colitis reveals nicotinic modulation of ion transport via iNOS-derived NO. Am J Physiol Gastrointest Liver Physiol 287: G706-G714, 2004

Grider JR, Jin JG. Distinct populations of sensory neurons mediate the peristaltic reflex elicited by muscle stretch and mucosal stimulation. J Neurosience 14: 2854-2860, 1994

Grundy D, Scratcherd T. Sensory afferents from the gastrointestinal tract. In: Wood JD, editor. Handbook of physiology, section 6, vol. 1, part 1. Bethesda, MD: American Physiological Society. p 593-620, 1989

Grundy D. Neuroanatomy of visceral nociception: vagal and splanchnic afferent. Gut 51: 2-5, 2002

Grynkiewicz G, Poenie M, Tsien RY. A new generation of Ca^{+2} indicators with greatly improved fluorescence properties. J Biol Chem 260: 3440-3450, 1985

Hanani M, Lasser-Ross N. Activity-dependent changes in intracellular calcium in myenteric neurons. Am J Physiol Gastrointest Liver Physiol. 273: G1359-G1363, 1997

Hendrisks R, Bornstein JC, Furness JB. An electrophysiological study of the projections of putative sensory neurons within the myenteric plexus of the guinea-pig ileum. Neurosci Lett 110: 286-290, 1990

Hess DT, Matsumoto A, Kim SO, Marshal HE, Stamler JS. Protein S-nitrosylation: Purview and parameters. Nat Rev Mol Cell Biol 6: 150-166, 2005

Hirooka K, Kourennyi DE, Barnes S. Calcium channel activation facilitated by nitric oxide in retinal ganglion cells. J Neurophysiol 83: 198-206, 2000

Hirst GDS, Holman ME, Spence I. Two types of neurones in the myenteric plexus of duodenum in the guinea-pig. J Physiol 236: 303:326, 1974

Hofmann F, Biel M, Flockerzi V. Molecualr basis for Ca^{2+} channel diversity. Annu Rev Neurosci 17: 399-418, 1994

Holst MC, Kelly JB, Powley TL. Vagal preganglionic projections to the enteric nervous system characterized with phaseolus vulgaris-leucoagglutinin. J Comp Neurol 381: 81-100, 1997

Hölzer HH, Raybould HE. Vagal and splanchnic sensory pathways mediate inhibition of gastric motility induced by duodenal distension. Am J Physiol 262: G603-608, 1992

Horiguchi K, Sanders KM, Ward SM. Enteric motor neurons from synaptic-like junctions with interstitial cells of Cajal in the canine gastric antrum. Cell Tissue Res 311: 299-313, 2003

Hu H, Chiamvimonvat N, Yamagishi T, Marban E. Direct inhibition of expressed cardiac L-type Ca^{2+} channels by S-nitrosothiol nitric oxide donors. Circ Res 81: 742-752, 1997

Huber A, Saur D, Kurjak M, Schusdziarra V, Allescher H. Characterization and splice variants of neuronal nitric oxide synthase in rat small intestine. Am J Physiol Gastrointest Liver Physiol 275: 1146-1156, 1998

Jacobowitz D. Histochemical studies of the autonomic innervation of the gut. J Pharmacol Exp Therap 149: 358-364, 1965

Janson G, Martinson J. Studies on the ganglionic site of action of sympathetic outflow to the stomach. Acta Physiol Scand 68: 184-192, 1966

Jiménez M, Borderies JR, Vergara P, Wang Y, Daniel EE. Slow waves in circular muscle of porcine ileum: structural and electrophysiological studies. Am J Physiol 276: G393-G406, 1999

Johnson SM, Katayama Y, North RA. Slow synaptic potentials in neurones of the myenteric plexus. J Physiol 301: 505-516, 1980

Jones RM, Cartier GE, Mcintosh JM, Bulaj G, Farrar VE, Olivera BM. Composition and therapeutic utility of conotoxins from genus Conus. Exp Opin Ther Patents 11: 603-623, 2001

Katayama Y, North RA. Does substance P mediate slow synaptic excitation within the myenteric plexus? Nature 274: 387-388, 1978

Kennedy MB. Regulation of neuronal function by calcium. Trends Neurosci 12: 417-420, 1989

Kerr FW, Preshaw RM. Secretomotor function of the dorsal motor nucleus of the vagus. J Physiol 205: 405-415, 1969

Kilbinger H, Wolf D. Increase by NO synthase inhibitors of acetylcholine release from guinea-pig myenteric plexus. Naunyn-Schmiedeberg's Arch Pharmacol 349: 543-545, 1994

Kimura H, Hokari R, Miura S, Shigematsu T, Hirokawa M, Akiba Y, Kurose I, Higuchi H, Fujimori H, Tsuzuki Y, Serizawa H, Ishiii H. Increased expression of inducible isoform of nitric oxide synthyse and the formation of peroxynitrite in colonic mucosa of patients with active ulcerative colitis. Gut 42: 180-187, 1998

Kirchgessner AL, Gershon MD. Identification of vagal efferent fibers and putative target neurons in the enteric nervous system of the rat. J Comp Neurol 285: 38-53, 1989

Kirchgessner AL, Liu MT. Differential localization of Ca^{2+} channel alpha1 subunits in the enteric nervous system: presence of alpha B channel-like immunoreactivity in intrinsic primary afferent neurons. J Comp Neurol 409: 85-104, 1999

Kochegarov AA. Pharmacological modulators of voltage-gated calcium channels and their therapeutical application. Cell Calcium 33: 145-162, 2003

Kuntz A, Saccomanno G. Reflex inhibition of intestinal motility mediated through decentralized prevertebral ganglia. J Neurophysiol 7: 163-170, 1944

Kunze WAA, Furness JB, Bertrand PP, Bornstein JC. Intracellular recording from myenteric neurons of the guinea-pig ileum that respond to stretch. J Physiol 506: 827-842, 1998

Lang RJ, Harvey JR, McPhee GJ, Klemm MF. Nitric oxide and thiol reagent modulation of Ca^{2+}-activated K^{+} channels in myocytes of the guinea-pig taenia caeci. J Physiol 525: 363-376, 2000

Langley JN, Magnus R. Some observations of movements of the intestine before and after degenerative section of the mesenteric nerves. J Physiol 33: 34-51, 1905

Langley JN. Connexions of the enteric nerve cells. J Physiol 56: 39, 1922

Larsson L. Immunocytochemistry: Theory and practice, CRC Press, Inc., Boca Raton, Florida, 1988

Lundberg JON, Hellstrom PM, Lundberg JM, Alving K. Greatly increased luminal nitric oxide in ulcerative colitis. Lancet 344: 1673-1674, 1994

Lundgren O. Sympathetic input into the enteric nervous system. Gut 47: 33-35, 2000

Mancinelli R, Fabrizi A, Vargiu R, Morrone L, Bagetta G, Azzena GB. Functional role of inducible nitric oxide synthase on mouse colonic motility. Neurosci Lett 311: 101-104, 2001

McDonough SI, Boland LM, Mintz IM, Bean BP. Interactions among toxins that inhibit N-type and P-type calcium channels. J Gen Physiol 119: 313-328, 2002

Mei N. Intestinal chemosensitivity. Physiol Rev 65: 221, 1985

Michel T, Lamas S. Molecular cloning of constitutive endothelial nitric oxide synthase: evidence for a family of related genes. J Cardiovasc Pharmacol 12: 45-49, 1992

Miller RJ. The control of neuronal Ca^{2+} homeostasis. Prog Neurobiol 37: 255-285, 1991

Mintz IM, Adams ME, Bean BP. P-type calcium channels in rat central and peripheral neurons. Neuron 9: 85–95, 1992

Moncada S, Palmer R MJ, Higgs EA. Biosynthesis of nitric oxide from L-arginine, a pathway for the regulation of cell function and communication. Biochem Pharmacol 38: 1709-1715, 1989

Moncada S, Palmer RMJ, Higgs EA. Nitric oxide: Physiology, pathophysiology, and pharmacology. Pharmacol Rev 43: 109-142, 1991

Moncoq K, Trieber CA, Young HS. The molecular basis for cyclopiazonic acid inhibition of the sarcoplasmic reticulum calcium pump. J Biol Chem 282: 9748-9757, 2007

Mullis KB, Faloona FH. Specific synthesis of DNA in vitro via a polymerase-catalyzed chain reaction. Methods Enzymol 155: 335-350, 1987

N´Gouemo P, Morad M. Voltage-gated calcium channels in adult rat inferior colliculus neurons. Neuroscience 120: 815-826, 2003

Nakao K, Takahashi T, Utsunomiya J, Owyang C. Extrinsic neural control of oxide synthase expression in the myenteric plexus of rat jejunum. J Physiol 507: 549-560, 1998

Nemeth PR, Zafirov D, Wood JD. Forskolin mimics slow synaptic excitation in myenteric neurons. Eur J Pharmacol 101: 303-304, 1984

Newton CR, Graham A. PCR. Intoduction to scientific techniques. 2d. ed. BIOS scientific publishers Ltd.,Oxford, 1997

Nishi S, North RA. Intracellular recording from the myenteric plexus of the guinea-pig ileum. J Physiol 231: 471-491, 1973

Noll S, Schaub-Kuhnen S. Praxis der Immunhistochemie. 1. ed. Urban und Fischer, München, 2000

Nonidez JF. Afferent nerve endings in the ganglia of the intermuscular plexus of the dog's esophagus. J Comp Neurol 85: 177-185, 1946

Nooney JM, Lambert RC, Feltz A. Identifying neuronal non-L Ca^{2+} channels; more than stamp collecting? Trends Pharmacol Sci 18: 363-371, 1997

North RA. Electrophysiology of the enteric nervous system. Neuroscience 7: 315-325, 1982

Palmer RM, Ferrige AG, Moncada S. Nitric oxide release accounts for the biological activity of endothelium-derived relaxing factor. Nature 327: 524-526, 1987

Palmer RM, Moncada S. A novel citruline-forming enzyme implicated in the formation of nitric oxide by vascular endothelial cells. Biochem Biophys Res Cummun 158: 348-352, 1989

Pavlick KP, Laroux FS, Fuseler J, Wolf RE, Gray L, Hoffman J, **Grisham MB**. Serial review: Reactive oxygen and nitrogen in inflammation. Free Rad Biol Med 33: 311-322, 2002

Pelzer D, Pelzer S, McDonald TF. Properties and regulation of calcium channels in muscle cells. Rev Physiol Biochem Pharmacol 114: 108-206, 1990

Petzold GC, Scheibe F, Braun JS, Freyer D, Priller J, Dirnagl U, **Dreier JP**. Nitric oxide modulates calcium entry through P/Q-type calcium channels and N-methyl-D-aspartate receptors in rat cortical neurons. Brain Research 1063: 9–14, 2005

Phillips RJ, Baronowsky EA, Powley TL. Afferent innervation of gastrointestinal tract smooth muscle by the hepatic branch of the vagus. J Comp Neurol 384: 248-270, 1997

Pilipenko VI. Contributions to the functional morphology of the peripheral nervous system. Part II. Functional nature of Dogiel's type II cells. Bull Exp Biol Med 41: 449-452, 1956

Powley TL, Holst MC, Boyd DB, Kelly JB. Three dimensional reconstructions of autonomic projections to the gastrointestinal tract. Microsc Res Technol 29: 297-309, 1994

Powley TL, Phillips RJ. Musing on the wanderer. What's new in our understanding of vago-vagal reflexes? I. Morphology and topogaphy of vagal afferents innervating the GI tract. Am J Physiol Gastrointest Liver Physiol 283: G1217-G1225, 2002

Powley TL. Vagal input to the enteric nervous system. Gut 47: 30-32, 2000

Prechtl JC, Powley TL. The fibers composition of the abdominal vagus of the rat. Anat Embryol 181: 101-115, 1990

Publicover NG, Hammond EM, Sanders KM. Amplification of nitric oxide signaling by interstitial cells isolated from canine colon. Proc Natl Acad Sci USA 90: 2087–2091, 1993

Quintana E, Hernández C, Álvarez-Barrientos A, Esplugues JV, Barrachina MD. Synthesis of nitric oxide in postganglionic myenteric neurons during endotoxemia: implications for gastric motor function in rats. FASEB J 18: 531-533, 2004

Regan LJ. Voltage-dependent calcium currents in Purkinje cells from rat cerebellar vermis. J Neurosci 11: 2259–2269, 1991

Rehn M, Hübschle T, Diener M. TNF-α hyperpolarises membrane potential and potentiates the response to nicotinic receptor stimulation in cultured rat myenteric neurons. Acta Physiol Scand 181: 13-22, 2004

Ritter RC, Brenner L, Yox DP. Participation of vagal sensory neurons in putative satiety signals from upper gastrointestinal tract. In: Ritter S, Ritter RC, Barnes CD(eds) Neuroanatomy and physiology of abdominal vagal afferents. CRC Press, Boca Raton, Ann Arbor, Boston, pp 221-248, 1992

Rodrigo J, Hernàndez CJ, Vidal MA, Pedrosa JA. Vegetative innervation of the esophagus. II Intraganglionic laminar endings. Acta Anat 92: 79-100, 1975

Roman C, Gonella J. Extrinsic control of digestive motility. In L.R. Johnson, J. Christensen, M.J. Jackson, E.D. Jacobson and J.H. Walsh(eds): Physiology of the Gastrointestinal Tract, Vol. 1. New York: Raven Press pp 507-553, 1987

Roony TA, Joseph SK, Queen C, Thomas AP. Cyclic GMP induces oscillatory calcium signals in rat hepatocytes. J Biol Chem 271: 19817-19825, 1996

Rühl A, Collins SM. Role of nitric oxide in norepinephrine release from myenteric plexus in vitro and in Trichinella spiralis-infected rats. Neurogastroenterol Motil 9: 33–39, 1997

Saiki RK, Scharf S, Faloona F, Mullis KB, Horn GT, Erlich HA, Arnheim N. Enzymatic amplification of beta-globin genomic sequences and restriction site analysis for diagnosis of sickle cell anemia. Science 230: 1350-1354, 1985

Sambrook J, Fritsch EF, Maniatis T. Molecular Cloning: a laboratory manual 2nd. Ed. New York:Cold Spring Harbor Laboratory Press, 1989

Sanders KM, Ward SM. Nitric oxide as a mediator of nonadrenergic noncholinergic neurotransmission. Am J Physiol Gastrointest Liver Physiol 262: G379-G392, 1992

Sanders KM. A case for interstitial cells of Cajal as pacemakers and mediators of neurotransmission in the gastrointestinal tract. Gastroenterology 111:492-515,1996

Sanguinetti MC, Kass RS. Voltage-dependent block of calcium channel current in calf purkinje fiber by dihydropyridine calcium channel antagonists. Circ Res 55: 336-348, 1984

Santiago AR, Carvalho CM, Carvalho AP, Ambrósio AF. Differential Contribution of L-, N-, and P/Q-type calcium channels to $[Ca^{2+}]_i$ changes evoked by kainate in hippocampal neurons. Neurochem Res 33: 1501-1508, 2008

Schäfer KH, Saffrey MJ, Brunstock G, Mestres-Ventura P. A new method for the isolation of myenteric plexus from the newborn rat gastrointestinal tract. Brain Res Protoc 1: 109-113, 1997

Schäufele N, Diener M. Pharmacological characterisation of voltage-dependent Ca^{2+} channels in isolated ganglia from the myenteric plexus. Life Scie 77: 2489–2499, 2005

Schemann M, Grundy D. Electrophysiological identification of vagally innervated enteric neurons in guinea pig stomach. Am J Physiol 263: G709-G718, 1992

Schemann M, Wood JD. Synaptic behavior of myenteric neurons in the gastric corpus of the guinea-pig. J Physiol 417: 519-535, 1989

Schricker K, Pötzl B, Hamann M, Kurtz A. Coordinate changes of renin and brain-type nitric-oxide-synthase (b-NOS) mRNA levels in rat kidneys. Pflügers Arch Eur J Physiol 432: 394-400, 1996

Schultheiss G, Seip G, Kocks SL, Diener M. Ca^{2+}-dependent and Ca^{2+}-independent Cl^- secretion stimulated by the nitric oxide donor, GEA 3162, in rat colonic epithelium. Eur J Pharmacol 444: 21-30, 2002

Sharp PA, Suqden B, Sambrook J. Detection of two restriction endonuclease activities in haemophilus parainfluenza using analytical agarose-ethidium bromide electophoresis. Biochemistry 12: 3055-3063, 1973

Sher E, Biancardi E, Passafaro M, Clementi F. Physiopathology of neuronal voltage-operated calcium channels. FASEB J 5: 2677-2683, 1991

Simpson PB, Challis RAJ, Nahorski SR. Neuronal Ca^{2+} stores: activation and function. Trends Neurosci 18: 299-306, 1995

Sitmo M, Rehn M, Diener M. Stimulation of voltage-dependent Ca^{2+} channels by NO at rat myenteric neurons. Am J Physiol Gastrointest Liver Physiol 293: G886-G893, 2007

Smith GP, Rauhofer EA, Gibbs J. CCK-8 inhibits meal size in rats that have only the hepatic-dudenal vagal branch intact 1995. Benjamin Franklin/Lafayette Symphaguik (abstract). Appetite 24: 93, 1994

Smith TK, Reed JB, Sanders KM. Electrical pacemakers of canine proximal colon are functionally innervated by inhibitory motor neuronsn. Am J Physiol 256: C466-C477, 1989

Stolovitzky G, Cecchi G. Efficiency of DNA replication in the polymerase chain reaction. Proc Nat Acad Sci USA 93: 12947-12952, 1996

Surprenant A, North RA. Mechanism of synaptic inhibition by noradrenaline acting at alpha 2-adrenoceptors. Proc R Soc Lond 234: 85-114, 1988

Takahashi T. Pathophysiological significance of neuronal nitric oxide synthase in the gastrointestinal tract. Gastroenterology 38: 421-430, 2003

Tamura K, Schemann M, Wood JD. Actions of nitric oxide-generating sodium nitroprusside in myenteric plexus of guinea pig small intestine. Am J Physiol 265: G887–G893, 1993

Thornbury KD, Ward SM, Dalziel HH, Carl A, Westfall DP, Sanders KM. Nitric oxide and nitrosocysteine mimic nonadrenergic, noncholinergic hyperpolarization in canine proximal colon. Am J Physiol Gastrointest Liver Physiol 261: G553-G557, 1991

Thuneberg L. Interstitial cells of Cajal: Intestinal pacemaker cells? Adv Anat Embryol Cell Biol 71: 1-130, 1982

Triggle DJ. Calcium channel antagonists: Clinical uses: Past, present and future. Biochem Pharmacol 74: 1-9, 2007

Tringham EW, Dupere JRB, Payne CE, Usowicz MM. Protease treatment of cerebellar Purkinje cells renders ω-Agatoxin IVA-sensitive Ca^{2+} channels insensitive to inhibition by ω-conotoxin GVIA. J Pharmacol Exp Therap 324: 806-808, 2008

Tsien RY, Rink TJ, Poenie M. Measurement of cytosolic free Ca^{+2} in individual small cells using fluorescence microscopy with dual excitation wavelengths. Cell Calcium 6: 145-157, 1985

Tsien RY. A non-disruptive technique for loading calcium buffers and indicators into cells. Nature 290: 527-528, 1981

Tsien RY. Fluorescent probes of cell signaling. Ann Rev Neurosci 12: 227-253, 1989

Tsien RY. New calcium indicators and buffers with high selectivity against magnesium and protons: Design, synthesis, and properties of prototype structures. Biochemistry 19: 2396-2404, 1980

Valentine JF, Tannahill CL, Stevenot SA, Sallustio JE, Nick HS, Eaker EY. Colitis and interleukin 1β up-regulation inducible nitric oxide synthase and superoxide dismutase in rat myenteric neurons. Gastroenterology 111: 56-64, 1996

Vallance BA, Dijkstra G, Qiu B, van der Waaij LA, van Goor H, **Jansen PLM, Mashimo H, Collins SM**. Relative contributions of NOS isoforms during experimental colitis: endothelial-derived NOS maintains mucosal integrity. Am J Physiol Gastrointest Liver Physiol 287: G865-G874, 2004

Walls EK, Wang FB, Holst M-C, Phillips RJ, Powley TL. Suppression of meal size by intestinal nutrients is eliminated by celiac vagal deafferentation. Am J Physiol 269: R1410-R1419, 1995

Wang FB, Powley TL. Topographic inventories of vagal afferents in the gastrointestinal muscle. J Comp Neurol 421: 302-324, 2000

Wang FB, Powley TL. Toxonomy of vagal afferent projections to the gastrointestinal tract. Soc Neurosci Abstr 20: 1375, 1994

Wang Y, Marsden PA. Nitric oxide synthase: gene structure and regulation. Adv Pharmacol 43: 71-90, 1995

Wang ZQ, Watanabe Y, Toki A, kohno S, Hasegawa S, Hamazaki M. Involvement of endogenous nitric oxide and c-kit-expressing cells in chronic intestinal pseudo-obstruction. J Pediatr Surg 35: 539-544, 2000

Ward SM. Interstitial cells of Cajal in enteric neurotransmission. Gut 47: 40-43, 2000

Ward SM, Burns AJ, Torihashi S, Sanders KM. Mutation of the proto-oncogene c-kit blocks development of interstitial cells and electrical rhythmicity in murine intestine. J Physiol 480: 91-97, 1994

Wiklund CU, Olgart C, Wiklund NP, Gustafsson LE. Modulation of cholinergic and substance P-like neurotransmission by nitric oxide in the guinea-pig ileum. Br J Pharmacol 110: 833-839, 1993

Williams RM, Berthoud HR, Stead RH. Vagal afferent nerve fibers contact mast cells in rat small intestinal mucosa. Neuroimmunomodulation 4: 266-270, 1997

Wood JD, Mayer CJ. Serotonergic activation of tonic-type enteric neurons in guinea-pig small bowel. J Neurophysiol 42: 582-593, 1979

Wood JD. Enteric neuroimmunophysiology and pathophysiology. Gastroenterology 127: 635–657, 2004

Wood JD. Enteric neurophysiology. Am J Physiol 10: G585-G598, 1984

Wood JD. Physiology of the enteric nervous system. In L.R. Johnson (ed): Physiology of the gastrointestinal Tract.2nd Ed. New York: Raven Press, pp 67-109, 1987

Wood JD. Physiology of the enteric nervous system. In: Physiology of the Gastrointestinal Tract, Vol. 1, 3rd Edition. Hrsg.: Johnson LR, Raven Press, New York 423-482, 1994

Xie QW, Cho HJ, Calaycay J, Mumford RA, Swiderek KM, Lee TD, Ding A, Troso T, Nathan C. Cloning and characterization of inducible nitric oxide synthase from mouse macrophages. Science 256: 225-228, 1992

Yoshimura N, Seki S, de Groat WC. Nitric oxide modulates Ca^{2+} channels in dorsal root ganglion neurons innervating rat urinary bladder. J Neurophysiol 86: 304–311, 2001

Young HM, McConalogue K, Furness JB, DE Vente J. Nitric oxide targets in the guinea-pig intestine identified by induction of cyclic GMP immunoreactivity. Neuroscience 55: 583-596, 1993

Yuan SY, Bornstein JC, Furness JB. Pharmacological evidence that nitric oxide may be a retrograde messenger in the enteric nervous system. Brit J Pharmacol 114: 428-432, 1995

Zaitsev AV, Povysheva NV, Lewis DA, Krimer LS. P/Q-Type, but not N-type calcium channels mediate GABA release from fast-spiking interneurons to pyramidal cells in rat prefrontal cortex. J Neurophysiol 97: 3567-3573, 2007

8. Acknowledgments

I would like to express my sincere gratitude to my supervisor Prof. Dr. Martin Diener for his excellent guidance and for his great support, patience and enthusiasm during completion this study.

I specially acknowledge Dr. Matthias Rehn for his expert and practical help in data analysis.

I am grateful to Brigitta Brück for friendly help in PCR experiments.

Furthermore I wish to thank Anne Siefjediers, Eva-Maria Haas, Alice Metternich, Michael Haas, Silke Handstein, Daniela Hild, Karl-Hermann Maurer, Britta Henning, Bärbel Schmidt and all people in the Institute for Veterinary Physiology for various supports.

Surely my words will not encompass my thank and gratitude to my family for hearing, understanding, encouragment and most of all love even when they were so far away in moments I saw no light to go the way to the end.

9. Erklärung

Ich erkläre: Ich habe die vorgelegte Dissertation selbständig und ohne unerlaubte fremde Hilfe und nur mit den Hilfen angefertigt, die ich in der Dissertation angegeben habe. Alle Textstellen, die wörtlich oder sinngemäß aus veröffentlichten oder nicht veröffentlichten Schriften entnommen sind, und alle Angaben, die auf mündlichen Auskünften beruhen, sind als solche kenntlich gemacht. Bei den von mir durchgeführten und in der Dissertation erwähnten Untersuchungen habe ich die Grundsätze guter wissenschaftlicher Praxis, wie sie in der „Satzung der Justus-Liebig-Universität Gießen zur Sicherung guter wissenschaftlicher Praxis“ niedergelegt sind, eingehalten.

édition scientifique
VVB LAUFERSWEILER VERLAG

VVB LAUFERSWEILER VERLAG
STAUFENBERGRING 15
D-35396 GIESSEN

Tel: 0641-5599888 Fax: -5599890
redaktion@doktorverlag.de
www.doktorverlag.de

ISBN 3-8359-5386-9